COMPUTER METHODS IN APPLIED MECHANICS AND ENGINEERING 81 (1990) 91–126
NORTH-HOLLAND

ON A STRESS RESULTANT GEOMETRICALLY EXACT SHELL MODEL. PART IV: VARIABLE THICKNESS SHELLS WITH THROUGH-THE-THICKNESS STRETCHING

J.C. SIMO, M.S. RIFAI and D.D. FOX
Division of Applied Mechanics, Department of Mechanical Engineering, Stanford University, Stanford, CA, U.S.A.

Recieved date 23 June 1989

This paper is concerned with the extension of the shell theory and numerical analysis presented in Parts I, II and III to include finite thickness stretch and initial variable thickness. These effects play a significant role in problems involving finite membrane strains, contact, concentrated surface loads and delamination (in composite shells). We show that a direct numerical implementation of the standard single extensible director shell model circumvents the need for rotational updates, but exhibits numerical ill-conditioning in the thin shell limit. A modified formulation obtained via a multiplicative split of the director field into an extensible and inextensible part is presented, which involves only a trivial modification of the weak form of the equilibrium equations considered in Part III, and leads to a perfectly well-conditioned formulation in the thin-shell limit. In sharp contrast with previous attempts in the context of the degenerated solid approach, the thickness stretch is an independent field, not a dependent variable updated iteratively via the plane stress condition. With regard to numerical implementation, an exact update procedure which automatically ensures that the thickness stretch remains positive is presented. For the present theory, standard displacement models would exhibit 'locking' in the incompressible limit as a result of the essentially three-dimensional character of the constitutive equations. A mixed formulation is described which circumvents this difficulty. Numerical examples are presented that illustrate the effects of the thickness stretch, the performance of the proposed mixed interpolation, and the well-conditioned response exhibited by the present approach in the thin-shell (inextensible director) limit.

1. Introduction

In [1–3] (henceforth referred to as Parts I, II and III of this work), a non-linear geometrically exact stress resultant shell model for the analysis of large deformations in shell structures is presented, along with a detailed discussion of computational aspects within the context of the finite element method. This formulation is based on the classical kinematic hypothesis which defines a point in the shell by the mid-surface position vector $\varphi(\xi^1, \xi^2)$, where $(\xi^1, \xi^2) \in \mathscr{A}$, and a distance $\xi \in [h_-, h_+]$ along a unit vector $t(\xi^1, \xi^2)$. Due to the presence of transverse shear deformation, this unit vector, often referred to as the director field, does not necessarily coincide with the normal vector to the mid-surface (see Fig. 2.1). Such an assumption precludes thickness changes and cannot accommodate initial variable thickness—two effects which play an important role in applications involving finite membrane strains, contact, localized effects due to concentrated surface loading and delamination of

composite shells, among others. This paper is concerned with the extension of our theoretical and numerical analysis in Parts I, II and III, to include the effects of thickness change and initial variable thickness. We show that this extension amounts to the addition of an extra term, with a remarkably simple functional form, to the weak form of the momentum balance equations from the inextensible director theory.

Linear shell theories involving various degrees of approximation and aimed at accounting for thickness change date back at least to the pioneering work of Hildebrand et al. [4] and Green and Zerna [5]. For a historical review up to 1970, we refer to [6, Sections 20, 21]. Nonlinear extensions of the classical Reissner–Meissner axisymmetric shell equations accounting for thickness stretch are given in [7] and references therein. Presently, within the context of the general nonlinear theory, the local form of the balance equations incorporating thickness stretch is well established; see e.g. [6, eqs. (9.13), (9.21) and (9.23)]. An essential feature of these equations, often overlooked in the classical literature and emphasized in Part I, is that either in local or in weak form, they can be phrased in vector notation in such a way that explicit appearance of covariant derivatives associated with the Riemannian connection on the mid-surface are avoided. This point of view, also adopted by Antman [8], is crucial to the numerical implementation of classical shell theory.

Conceptually, the effects of thickness change can be included in classical shell models in a straightforward fashion. One merely replaces the unit director field $t(\xi^1, \xi^2)$ with an extensible director field, now denoted by $d(\xi^1, \xi^2)$, whose length $\lambda := \|d\| > 0$ accounts for the thickness stretch. From a mechanical standpoint, this enhanced kinematic assumption leads to the explicit appearance of three new stress resultants not otherwise present in classical shell models: the normal or through-the-thickness stress resultant $\tilde{l}^3$ and two additional bending couples $\tilde{m}^{3\alpha}$ ($\alpha = 1, 2$). For linear isotropic elastic reponse, explicit constitutive equations for these stress resultants are given in [9].

From a numerical analysis point of view, we show below that this class of models, referred to as the standard extensible director formulation in what follows, possesses a very attractive feature; namely, rotational updates associated with the (classical) inextensible director formulation are entirely by-passed. In fact, the update procedure consistent with the standard extensible director theory simply reduces to vector addition. However, as our numerical simulations demonstrate, such a direct implementation of the extensible director model leads to a numerical formulation which is ill-conditioned in the thin shell limit. This difficulty can be traced to the fact that the inextensibility condition of the director field in the thin shell limit is effectively enforced by a penalty procedure which becomes progressively ill-conditioned as the thickness tends to zero.

We show that the ill-conditioning of the formulation can be circumvented by introducing a multiplicative decomposition of the (extensible) director field into an inextensible vector part and a scalar stretching part. For axisymmetric shells, a similar technique is employed in [10, eqs. (1.3)–(1.5)] and for linear shells an analogous reparametrization is used in [9]. Remarkably, the resulting formulation is completely general and the weak form of the momentum equations involves only a trivial modification of the classical inextensible director theory considered in Parts I and III. Essentially, this modification entails only the addition of a term involving the logarithmic stretch of the director field. We remark that this formulation is at variance with previous attempts in the context of the degenerated solid approach, where the thickness change is accounted for via a staggered iterative update procedure constructed by

exploiting the plane–stress assumption; see e.g. [11]. By contrast, in the present approach, the thickness stretch is truly an independent field coupled to the bending, membrane and transverse shear fields. This feature is vital in many applications where the localized effects of thickness change trigger important variations in the solutions (e.g., composite delamination, crack propagation).

A crucial advantage of shell models incorporating thickness stretch lies in the simplicity involved in implementing fully three-dimensional constitutive models. In sharp contrast with the classical inextensible director theory, formulations employing an extensible director do not require the explicit enforcement of the plane stress assumption at the outset. As a result, three-dimensional type constitutive relations can be used. In particular, we have been able to incorporate classical three-dimensional elasticity models, such as Neo-Hookean and Mooney–Rivlin materials, entirely in a stress resultant format. Furthermore, as demonstrated by our numerical experiments, plane stress response is recovered automatically in the thin-shell limit without a trace of ill-conditioning. From a numerical standpoint, however, the effective exploitation of this feature requires careful design of the finite element interpolations in order to avoid the well-known locking phenomenon exhibited by standard displacement models in the incompressible limit. A mixed finite element interpolation that circumvents these difficulties is also developed. For simplicity, this paper will be restricted to a classical quadratic isotropic stored energy function (of the St. Venant–Kirchhoff type) with the through-the-thickness stress resultant linearly related to the logarithmic stretch, although the theory allows for the use of any three-dimensional hyper-elastic material model. A formulation incorporating finite stress plasticity within the context of the inextensible director is presented in [12].

An outline of the rest of this paper is as follows: In Section 2 we summarize the kinematic description of the shell allowing for thickness change, along with the basic equations of the standard single extensible director formulation in both local (strong) and global (weak) form. In Section 3 we reparametrize these equations in terms of a thickness stretch field and an inextensible director field via a multiplicative decomposition of the extensible director. The effects of external surface loads are considered in detail, and the contributions to the weak form are presented along with their linearization. We show that, in general, surface loads result in contributions to both the displacement and the rotational degrees of freedom. The importance of properly accounting for these contributions is illustrated numerically in Section 5. We conclude Section 3 with an example of a simple constitutive model that generalizes the standard quadratic stored energy function employed in classical shell theory and illustrates the three-dimensional character of the constitutive equations inherent to the present formulation.

Finite element and numerical analysis aspects are examined in Section 4. First, within the context of the reparametrized shell theory introduced in Section 3, we consider the matrix formulation of the weak form of the equilibrium equations, along with a mixed formulation of the constitutive equations. These variational equations constitute the basis for our mixed finite element interpolation discussed subsequently. Next, we consider the iterative solution procedure and develop an exact update procedure for the thickness stretch which complements our rotational updates discussed in detail in Part III. The thickness stretch update algorithm relies crucially on the use of the logarithmic stretch. The update is additive and, via the exponential map, automatically enforces the condition that the updated stretch is positive. We conclude Section 4 with an outline of the numerical implementation of the standard extensible director formulation summarized in Section 2, and show that rotational updates are not necessary

within this framework. However, as alluded to before, despite its conceptual appeal, this formulation suffers from ill-conditioning in the thin-shell limit and, in its present form, can only be used for thick shell analysis. In Section 5 several numerical examples are presented which demonstrate the behavior of the present formulation and its finite element implementation both in the thin shell and in the incompressible limits. Illustrative examples are also presented for finite deformations. Conclusions are drawn in Section 6.

2. Governing equations accounting for thickness stretch

In this section, we summarize the basic kinematic description of nonlinear shell theory incorporating thickness stretch and outline the exact balance equations formulated in terms of stress resultants and stress couples. We close this section with the statement of the weak form of the equilibrium equations. Once more we emphasize that these balance equations are cast in a vector format which does not explicitly involve covariant derivatives associated with the Riemannian connection on the mid-surface (compare e.g. with [6]). A reparametrization of these equations that avoids numerical ill-conditioning in the thin-shell (inextensible director) limit is introduced in Section 3.

2.1. Kinematic description of the shell

Points in the shell are parametrized by a system of coordinates $(\xi^1, \xi^2, \xi) \in \mathscr{A} \times \mathscr{I}$, where $\xi^3 = \xi \in \mathscr{I}$ is the through-the-thickness coordinate; $\mathscr{A}$ and $\mathscr{I} = [h_-, h_+]$ are fixed regions in $\mathbb{R}^2$ and $\mathbb{R}$, respectively. Any placement $\mathscr{S} \subset \mathbb{R}^3$ of the shell in Euclidean space is then defined by a mapping $\hat{\boldsymbol{\Phi}} : \mathscr{A} \times \mathscr{I} \to \mathbb{R}^3$ as

$$\mathscr{S} := \{x \in \mathbb{R}^3 \mid x = \hat{\boldsymbol{\Phi}}(\xi^1, \xi^2, \xi) \text{ for } (\xi^1, \xi^2, \xi) \in \mathscr{A} \times \mathscr{I}\} . \tag{2.1}$$

The basic kinematic hypothesis underlying shell theory concerns the form of the mapping $\hat{\boldsymbol{\Phi}}(\xi^1, \xi^2, \xi)$. According to the standard single extensible director assumption, one assumes that an arbitrary point x in any placement of the shell $\mathscr{S}$ can be identified as

$$x = \hat{\boldsymbol{\Phi}}(\xi^1, \xi^2, \xi) := \boldsymbol{\varphi}(\xi^1, \xi^2) + \xi \boldsymbol{d}(\xi^1, \xi^2) . \tag{2.2}$$

Here, $\boldsymbol{\varphi} : \mathscr{A} \to \mathbb{R}^3$ defines the mid-surface of the shell in $\mathscr{S}$, and $\boldsymbol{d} : \mathscr{A} \to \mathbb{R}^3$ the director field (or thickness fiber). However, in contrast with our developments in Part III, we no longer assume that $\boldsymbol{d}(\xi^1, \xi^2)$ is of unit length. Instead, we only require that

$$\lambda(\xi^1, \xi^2) := \|\boldsymbol{d}(\xi^1, \xi^2)\| > 0 \quad \text{for } (\xi^1, \xi^2) \in \mathscr{A} . \tag{2.3}$$

In what follows, we shall refer to $\lambda : \mathscr{A} \to \mathbb{R}_+$ defined by (2.3) as the thickness stretch; see Fig. 2.1. The abstract configuration space $\mathscr{C}$ associated with the kinematic assumption (2.2) is therefore given by

$$\mathscr{C} = \{\boldsymbol{\Phi} = (\boldsymbol{\varphi}, \boldsymbol{d}) : \mathscr{A} \to \mathbb{R}^3 \times \mathbb{R}^3 \mid \boldsymbol{d} \cdot [\boldsymbol{\varphi}_{,1} \times \boldsymbol{\varphi}_{,2}] > 0\} . \tag{2.4a}$$

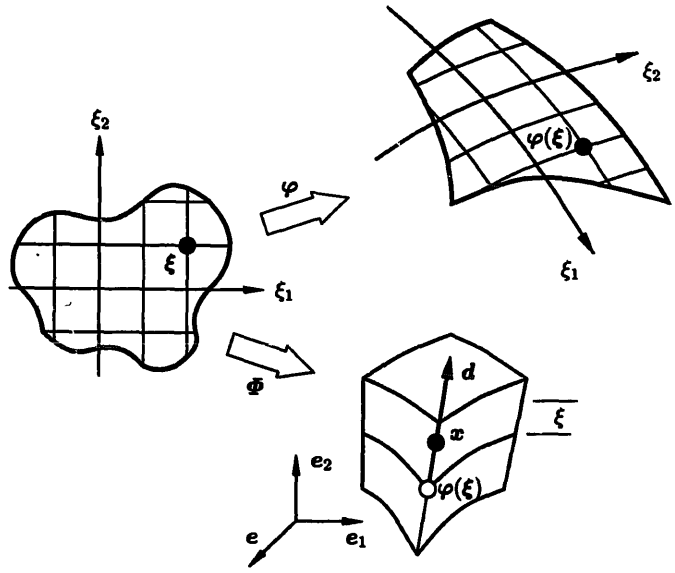

Fig. 2.1. Kinematic assumption for the inextensible and extensible formulations. Any point in the shell configuration is defined by its position φ on the mid-surface and a distance ξ along a director d. The inextensible formulation enforces the condition $\|d\| = 1$, whereas in the present extensible formulation $\|d\| > 0$ is an additional kinematic variable defining the configuration.

Note that the condition $d \cdot [\varphi_{,1} \times \varphi_{,2}] > 0$ precludes the physically unreasonable situation of infinite transverse shearing. We subject the configurations $\Phi \in \mathscr{C}$ to displacement-like (Dirichlet) boundary conditions defined by the relations

$$\varphi|_{\partial_\varphi \mathscr{A}} = \tilde{\varphi} \text{ (given)} \quad \text{and} \quad d|_{\partial_d \mathscr{A}} = \tilde{d} \text{ (given)}, \tag{2.4b}$$

where $\partial_\varphi \mathscr{A}$ and $\partial_d \mathscr{A}$ are the parts of the boundary where the mid-surface displacement and the director field are prescribed, respectively.

2.2. *Stress resultants, stress couples and balance laws*

As in Part III, we denote by n^α, $\tilde{m}^\alpha$ and l the resultant stress, resultant couple stress and resultant through-the-thickness stress (Fig. 2.2). In components relative to the (convected) basis

$$\{a_1, a_2, a_3\} = \{\varphi_{,1}, \varphi_{,2}, d\}, \tag{2.5a}$$

these resultants are given by

$$\begin{aligned} n^\alpha &= n^{\beta\alpha}\varphi_{,\beta} + q^\alpha d, && \text{(resultant stress)} \\ \tilde{m}^\alpha &= \tilde{m}^{\beta\alpha}\varphi_{,\beta} + \tilde{m}^{3\alpha} d, && \text{(resultant stress couple)} \\ l &= l^\alpha \varphi_{,\alpha} + l^3 d && \text{(through-the-thickness stress)}. \end{aligned} \tag{2.5b}$$

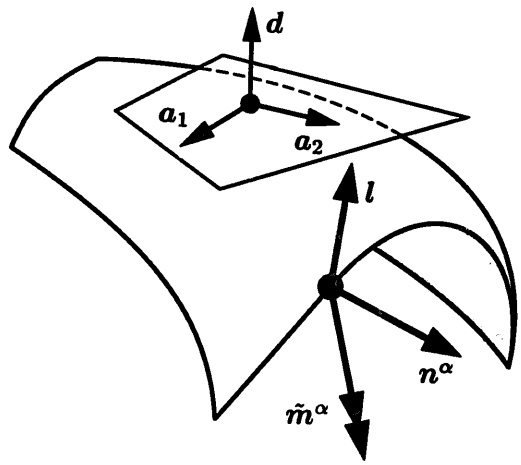

Fig. 2.2. Convected (mid-surface) basis, stress resultants, resultant stress couples, and through-the-thickness stress resultant.

The local form (or strong form) of the equilibrium equations in terms of the stress and stress couple resultants in (2.5) can be written

$$\frac{1}{\bar{j}}(\bar{j}n^\alpha)_{,\alpha} + \bar{n} = 0\,, \qquad \frac{1}{\bar{j}}(\bar{j}\tilde{m}^\alpha)_{,\alpha} - l + \bar{m} = 0\,. \tag{2.6}$$

A detailed derivation of these equations and the definition of the applied loads $\bar{n}$ and $\bar{m}$ is given in Part I. Equations (2.6) are the resultant balance of linear momentum and balance of director momentum (equivalent to balance of couples around the mid-surface), respectively. The balance of angular momentum equation (equivalent to $\sigma = \sigma^t$ in the three-dimensional theory) is written as

$$n^\alpha \times \varphi_{,\alpha} + \tilde{m}^\alpha \times d_{,\alpha} + l \times d = 0\,. \tag{2.7}$$

Equations (2.6) and (2.7) along with a suitable set of constitutive equations form a complete system of field equations governing the present shell model. The external loading terms $\bar{n}$ and $\bar{m}$ are defined in Appendix A of Part I and will be elaborated on further in Section 3.3.

2.3. *Effective stress resultants*; *balance of angular momentum*

The balance of angular momentum equation, as given by (2.7), can be satisfied a priori by expressing the balance laws in terms of modified (effective) stress resultants as follows. Define the effective stress resultant tensor $\tilde{n}$ by the expression

$$\tilde{n} := n^\alpha \otimes \varphi_{,\alpha} + l \otimes d - d_{,\alpha} \otimes \tilde{m}^\alpha\,. \tag{2.8a}$$

Using standard vector product identities, it can be easily shown that symmetry of $\tilde{n}$ is equivalent to (2.7); namely, the following equivalence holds:

$$\text{Balance of angular momentum} \;\Leftrightarrow\; \tilde{n} = \tilde{n}^t\,. \tag{2.8b}$$

The effective resultant $\tilde{\boldsymbol{n}}$ plays the role of the Cauchy stress tensor $\boldsymbol{\sigma}$ from the three-dimensional theory.

The symmetry condition (2.8b) admits a simple mechanical interpretation when expressed in component form. Resolve $\boldsymbol{d}_{,\alpha}$ into components relative to the mid-surface convected basis $\{\boldsymbol{a}_1, \boldsymbol{a}_2, \boldsymbol{a}_3\}$ according to (see Part I, eq. (4.21))

$$\boldsymbol{d}_{,\alpha} = \lambda_\alpha^\gamma \boldsymbol{\varphi}_{,\gamma} + \lambda_\alpha^3 \boldsymbol{d} . \tag{2.9}$$

From (2.8) and (2.9) we obtain the following component expression for the effective stress tensor $\tilde{\boldsymbol{n}}$ relative to the surface convected basis

$$\begin{aligned}
&\tilde{n}^{\alpha\beta} = n^{\alpha\beta} - \lambda_\gamma^\alpha \tilde{m}^{\beta\gamma} , && \text{(membrane)} \\
&\tilde{n}^{3\alpha} = q^\alpha - \lambda_\gamma^3 \tilde{m}^{\alpha\gamma} =: \tilde{q}^\alpha , && \text{(transverse shear)} \\
&\tilde{n}^{\alpha 3} = l^\alpha - \lambda_\gamma^\alpha \tilde{m}^{3\gamma} =: \tilde{l}^\alpha , && \text{(symmetric shear)} \\
&\tilde{n}^{33} = l^3 - \lambda_\gamma^3 \tilde{m}^{3\gamma} =: \tilde{l}^3 && \text{(across-thickness)} .
\end{aligned} \tag{2.10}$$

The equivalence relation (2.8b), in components, then takes the form

$$\text{Balance of angular momentum} \quad \Leftrightarrow \quad \tilde{n}^{\beta\alpha} = \tilde{n}^{\alpha\beta} \text{ and } \tilde{q}^\alpha = \tilde{l}^\alpha . \tag{2.11}$$

Note that the preceding definitions agree with those in Part I, Section 4.4.1. Next, we derive the weak form of the equilibrium equations (2.6) and express the result in terms of the effective resultants.

2.4. *Weak form of the equilibrium equations*

We start by defining the space of kinematically admissible variations associated with an arbitrary configuration $\boldsymbol{\Phi} \in \mathscr{C}$. Admissible variations consistent with the abstract configuration space (2.4), and hence consistent with the kinematic assumption (2.2), are given by

$$T_{\boldsymbol{\Phi}}\mathscr{C} = \{\delta\boldsymbol{\Phi} = (\delta\boldsymbol{\varphi}, \delta\boldsymbol{d}) : \mathscr{A} \to \mathbb{R}^3 \times \mathbb{R}^3 \mid \delta\boldsymbol{\varphi}|_{\partial_\varphi \mathscr{A}} = \boldsymbol{0}, \delta\boldsymbol{d}|_{\partial_d \mathscr{A}} = \boldsymbol{0}\} . \tag{2.12}$$

Next, by taking the dot product of the strong form (2.6) of the equilibrium equations with an arbitrary variation $\delta\boldsymbol{\Phi} \in T_{\boldsymbol{\Phi}}\mathscr{C}$, we obtain

$$\begin{aligned}
G(n^\alpha, \tilde{\boldsymbol{m}}^\alpha, \boldsymbol{l}; \delta\boldsymbol{\Phi}) = \int_{\mathscr{A}} \Big[&-\frac{1}{\bar{j}} (\bar{j}\boldsymbol{n}^\alpha)_{,\alpha} \cdot \delta\boldsymbol{\varphi} - \bar{\boldsymbol{n}} \cdot \delta\boldsymbol{\varphi} \\
&- \frac{1}{\bar{j}} (\bar{j}\tilde{\boldsymbol{m}}^\alpha)_{,\alpha} \cdot \delta\boldsymbol{d} + \boldsymbol{l} \cdot \delta\boldsymbol{d} - \bar{\boldsymbol{m}} \cdot \delta\boldsymbol{d} \Big] \bar{j} \, \mathrm{d}\xi^1 \, \mathrm{d}\xi^2 .
\end{aligned} \tag{2.13}$$

Making use of the divergence theorem, we obtain the following expression for the weak form of the equilibrium equations:

$$G(n^\alpha, \tilde{m}^\alpha, l; \delta\Phi) = \int_{\mathscr{A}} [n^\alpha \cdot \delta\varphi_{,\alpha} + \tilde{m}^\alpha \cdot \delta d_{,\alpha} + l \cdot \delta d]\, \bar{j}\, d\xi^1\, d\xi^2 - G_{\text{ext}}(\delta\Phi) = 0\,, \tag{2.14a}$$

where $G_{\text{ext}}(\delta\Phi)$ is the 'virtual work' expression associated with the external loading and given by

$$G_{\text{ext}}(\delta\Phi) := \int_{\mathscr{A}} [\bar{n} \cdot \delta\varphi + \bar{m} \cdot \delta d]\, \bar{j}\, d\xi^1\, d\xi^2 + \int_{\partial\mathscr{A}} [n^\alpha \cdot \delta\varphi + \tilde{m}^\alpha \cdot \delta d]\, \nu_\alpha \bar{j}\, d\Gamma\,. \tag{2.14b}$$

Next, we recast (2.14a) in terms of the (symmetric) effective stress resultants. Through a straightforward manipulation, essentially substituting component expressions (2.5b) and effective stress component expressions (2.10) into the weak form (2.14a), we arrive at the following expression:

$$\begin{aligned} G(\tilde{n}, \tilde{m}^\alpha, \Phi; \delta\Phi) = \int_{\mathscr{A}} [&\tilde{n}^{\alpha\beta} \varphi_{,\alpha} \cdot \delta\varphi_{,\beta} + \tilde{q}^\alpha (\varphi_{,\alpha} \cdot \delta d + \delta\varphi_{,\alpha} \cdot d) \\ &+ \tilde{m}^{\alpha\beta} (\varphi_{,\alpha} \cdot \delta d_{,\beta} + \delta\varphi_{,\alpha} \cdot d_{,\beta}) \\ &+ \tilde{m}^{3\alpha} (d \cdot \delta d_{,\alpha} + \delta d \cdot d_{,\alpha}) + \tilde{l}^3 d \cdot \delta d]\, \bar{j}\, d\xi^1\, d\xi^2 \\ &- G_{\text{ext}}(\delta\Phi) = 0\,. \end{aligned} \tag{2.15}$$

Expression (2.15) holds for any admissible variation $\delta\Phi \in T_\Phi \mathscr{C}$. To simplify our notation, the objects $\tilde{n}$ and $\tilde{m}^\alpha$ in the argument list for G are used to indicate the dependence of G on the components of these objects. From (2.15) we identify strain measure components defined by the relations

$$\begin{aligned} &\varepsilon_{\alpha\beta} = \tfrac{1}{2}(\varphi_{,\alpha} \cdot \varphi_{,\beta} - \varphi_{0,\alpha} \cdot \varphi_{0,\beta})\,, && \text{(membrane)} \\ &\tilde{\rho}_{\alpha\beta} = \varphi_{,\alpha} \cdot d_{,\beta} - \varphi_{0,\alpha} \cdot d_{0,\beta}\,, && \text{(bending)} \\ &\tilde{\delta}_\alpha = \varphi_{,\alpha} \cdot d - \varphi_{0,\alpha} \cdot d_0\,, && \text{(transverse shear)} \\ &\tilde{\chi}_\alpha = d_{,\alpha} \cdot d - d_{0,\alpha} \cdot d_0\,, && \text{(symmetric shear)} \\ &\tilde{\chi} = \tfrac{1}{2}(d \cdot d - d_0 \cdot d_0) && \text{(thickness stretch)}\,. \end{aligned} \tag{2.16}$$

It can be shown that these strain measure definitions give those components of the Lagrangian strain tensor from the three-dimensional theory, $E = \frac{1}{2}(F^t F - 1)$, which are either independent of the thickness parameter or linear in the through-the-thickness parameter ξ. Here, F is the deformation gradient $\nabla\hat{\Phi}\nabla\hat{\Phi}_0^{-1}$. The subscript $_0$ throughout refers to a quantity defined on the reference placement of the shell $\mathscr{S}_0$. We use a superposed $\tilde{}$ to differentiate the measures defined above from those reparameterized measures defined in Section 3 and used in the numerical implementation. With these definitions in hand, the weak form given by (2.15) can now be recast into the final component form as

$$G(\tilde{n}, \tilde{m}^{\alpha}, \Phi; \delta\Phi) = \int_{\mathscr{A}} [\tilde{n}^{\alpha\beta}\,\delta\varepsilon_{\alpha\beta} + \tilde{m}^{\alpha\beta}\,\delta\tilde{\rho}_{\alpha\beta} + \tilde{q}^{\alpha}\,\delta\tilde{\delta}_{\alpha} + \tilde{m}^{3\alpha}\,\delta\tilde{\chi}_{\alpha} + \tilde{l}^{3}\,\delta\tilde{\chi}]\,\bar{j}\,d\xi^{1}\,d\xi^{2} - G_{ext}(\delta\Phi) = 0\,. \tag{2.17}$$

In this expression, we have used the standard convention of writing $\delta(\cdot)$ to denote both a variation and the directional derivative of any of the strain measures $(\cdot)$ in the direction of the variation $\delta\Phi = (\delta\varphi, \delta d)$.

From a numerical analysis standpoint, the appeal of the formulation described so far lies in the simple structure taken by the space of variations. In contrast with the inextensible model employed in Part III, the removal of the inextensibility assumption on the director field (i.e. $\|d\| \neq 1$) leads to director variations which are no longer constrained to be tangent to the unit sphere (i.e. $d \cdot \delta d \neq 0$). This leads to the simple update procedure discussed in Section 4.4 which treats the director as an arbitrary vector in $\mathbb{R}^3$ and utilizes the linear structure of this space. Unfortunately, as demonstrated numerically in Section 5, this formulation results in severe numerical ill-conditioning in the thin-shell limit. An alternative kinematic description that circumvents this difficulty is considered next.

3. Reparametrization: multiplicative decomposition

By direct inspection of expressions (2.16) we conclude that the thickness stretch is coupled with both the bending and the shear measures. Therefore, deformations which produce large thickness changes can also result in large changes in the bending and shear strain measures $\tilde{\rho}_{\alpha\beta}$ and $\tilde{\delta}_{\alpha}$. To circumvent these undesirable features, we introduce a multiplicative decomposition of the director field into a magnitude parameter and a unit vector. As shown in Section 4, the resulting formulation only requires a straightforward modification of the inextensible formulation considered in Part III, and leads to a model which is well-conditioned in the thin-shell limit.

3.1. *Multiplicative decomposition of the director field*

We separate the stretching part of the director field from the inextensional part by setting

$$d(\xi^{1}, \xi^{2}) = \lambda(\xi^{1}, \xi^{2})\,t(\xi^{1}, \xi^{2})\,, \quad \text{with } \|t(\xi^{1}, \xi^{2})\| = 1 \text{ and } \lambda(\xi^{1}, \xi^{2}) > 0\,. \tag{3.1}$$

According to this multiplicative decomposition, we view the deformation of the director field as being composed of two parts: a rotation of the director field in the unit sphere given by the inextensional part $t: \mathscr{A} \to S^2$, followed by a stretching along t given by $\lambda: \mathscr{A} \to \mathbb{R}_+$; see Fig. 3.1. Equivalently, in place of the abstract configuration space (2.4a), we consider a configuration space now defined as

$$\mathscr{C} = \{\Phi = (\varphi, t, \lambda): \mathscr{A} \to \mathbb{R}^3 \times S^2 \times \mathbb{R}_+ \mid t \cdot [\varphi_{,1} \times \varphi_{,2}] > 0\}\,. \tag{3.2}$$

In terms of these alternative configuration variables, the relevant strain measures are

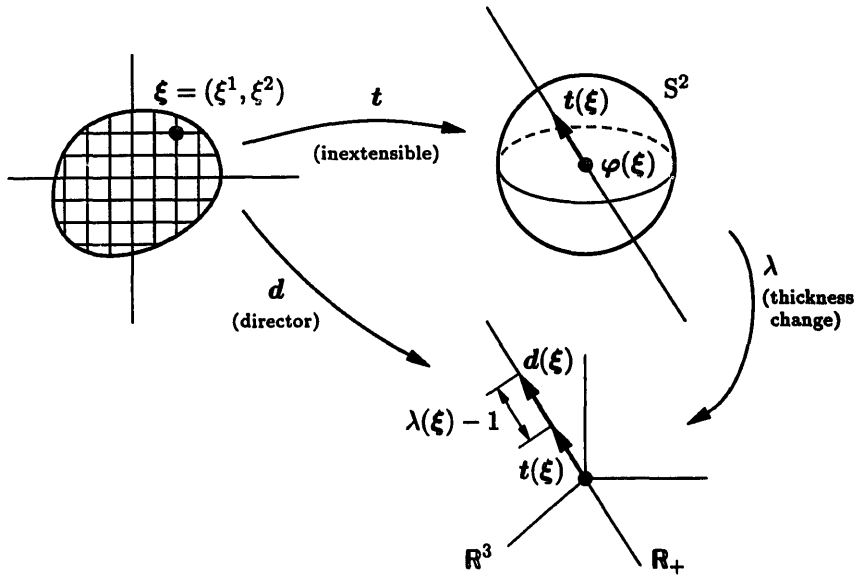

Fig. 3.1 Multiplicative decomposition of the director field into stretching and inextensible parts.

redefined as follows. The membrane, bending and transverse shear strains are defined in terms of the inextensible part of the director field exactly as in Part I and Part III. On the other hand, the stretching of the director field is defined in terms of logarithmic stretch according to the following expressions:

$$\begin{aligned} &\mu = \ln \lambda\,, && \text{(logarithmic stretch)} \\ &\mu_\alpha = \lambda_{,\alpha}/\lambda = \mu_{,\alpha} && \text{(logarithmic stretch gradient)}\,. \end{aligned} \tag{3.3}$$

The relevant strain measures using the reparameterization (multiplicative decomposition of the director field) are

$$\begin{aligned} &\varepsilon_{\alpha\beta} = \tfrac{1}{2}(\varphi_{,\alpha} \cdot \varphi_{,\beta} - \varphi_{0,\alpha} \cdot \varphi_{0,\beta})\,, && \text{(membrane)} \\ &\rho_{\alpha\beta} = \varphi_{,\alpha} \cdot t_{,\beta} - \varphi_{0,\alpha} \cdot t_{0,\beta}\,, && \text{(bending)} \\ &\delta_\alpha = \varphi_{,\alpha} \cdot t - \varphi_{0,\alpha} \cdot t_0\,, && \text{(transverse shear)} \\ &\chi_\alpha = (\ln \lambda)_{,\alpha} - (\ln \lambda_0)_{,\alpha} = \ln(\lambda/\lambda_0)_{,\alpha}\,, && \text{(logarithmic stretch gradient)} \\ &\chi = \ln \lambda - \ln \lambda_0 = \ln(\lambda/\lambda_0) && \text{(logarithmic stretch)}\,. \end{aligned} \tag{3.4}$$

The relationship between the preceding strain measures and those defined by (2.18) can be immediately established from the relation

$$d_{,\alpha} = \lambda[\mu_\alpha t + t_{,\alpha}]\,, \tag{3.5}$$

which follows from the multiplicative decomposition (3.1).

3.2. Modified weak form of the equilibrium equations

Our next step is to recast the weak form of the equilibrium equations in terms of the reparameterization introduced above. First, we observe that the space of admissible variations consistent with the abstract configuration space (3.2) is now given by

$$T_{\Phi}\mathscr{C} := \{\delta\Phi := (\delta\varphi, \delta t, \delta\lambda) : \mathscr{A} \to \mathbb{R}^3 \times T_t S^2 \times \mathbb{R} \mid \delta\varphi|_{\partial_\varphi \mathscr{A}} = \mathbf{0}\,,\ \delta t|_{\partial_t \mathscr{A}} = \mathbf{0}\,,\ \delta\lambda|_{\partial_\lambda \mathscr{A}} = 0\}\,. \tag{3.6}$$

In view of (3.1) and (3.3), director variations δd are related to thickness variations and inextensible director variations $(\delta\lambda, \delta t)$ by an expression analogous to (3.5); namely,

$$\delta d = \lambda[\delta\mu\, t + \delta t]\,, \quad \text{where } \delta\mu := \delta\lambda/\lambda\,. \tag{3.7}$$

Next, using (3.1) along with (3.5) and (3.7), a straightforward manipulation of the weak form (2.17) produces the following alternative expression:

$$G(\check{n}, \check{m}^\alpha, \Phi; \delta\Phi) = \int_{\mathscr{A}} [\check{n}^{\alpha\beta}\,\delta\varepsilon_{\alpha\beta} + \check{m}^{\alpha\beta}\,\delta\rho_{\alpha\beta} + \check{q}^\alpha\,\delta\delta_\alpha + \check{m}^{3\alpha}\,\delta\chi_\alpha + \check{l}^3\,\delta\chi]\,\bar{j}\,d\xi^1\,d\xi^2 - G_{\text{ext}}(\delta\Phi) = 0\,, \tag{3.8}$$

where $\delta\Phi = (\delta\varphi, \delta t, \delta\lambda) \in T_\Phi\mathscr{C}$ is an arbitrary admissible variation. The modified effective stress resultants in this variational equation (denoted by $\check{n}$ and $\check{m}^\alpha$ in the argument list) are defined in terms of the effective stress resultants and the resultant stress couple by the relations

$$\check{n}^{\alpha\beta} = \tilde{n}^{\alpha\beta}\,, \qquad \check{m}^{\alpha\beta} = \lambda\tilde{m}^{\alpha\beta}\,, \qquad \check{q}^\alpha = \lambda[\tilde{q}^\alpha + (\ln\lambda)_{,\beta}\tilde{m}^{\alpha\beta}]\,,$$
$$\check{m}^{3\alpha} = \tilde{m}^\alpha \cdot d\,, \qquad \check{l}^3 = l \cdot d + \tilde{m}^\alpha \cdot d_{,\alpha}\,. \tag{3.9}$$

In view of (3.8), with the exception of the last two terms of the integrand, the present extensible director formulation is identical to the inextensible theory of Part III. Hence, the extension of that theory to include the effects of thickness change only requires the addition of two terms to the weak form of the momentum balance equations.

3.3. Equivalent resultant (external) surface loads

It is common practice in the analysis of thin shells to assume that external forces are applied to the mid-surface of the shell configuration. Consequently, the effects of surface loads are often neglected. However, for thick shells, these effects are of considerable importance, especially in cases involving thickness stretch. As an example, pressure loads applied to the external surface affect the thickness of the shell much more dramatically than the same load applied to the mid-surface of the shell. Furthermore, surface loads produce a couple affecting the rotations of the inextensible director. The effects of loads applied to the surface can be derived through an examination of the external load contribution to the weak form as follows. For simplicity, we restrict our discussion to the case of zero body forces and dead loading.

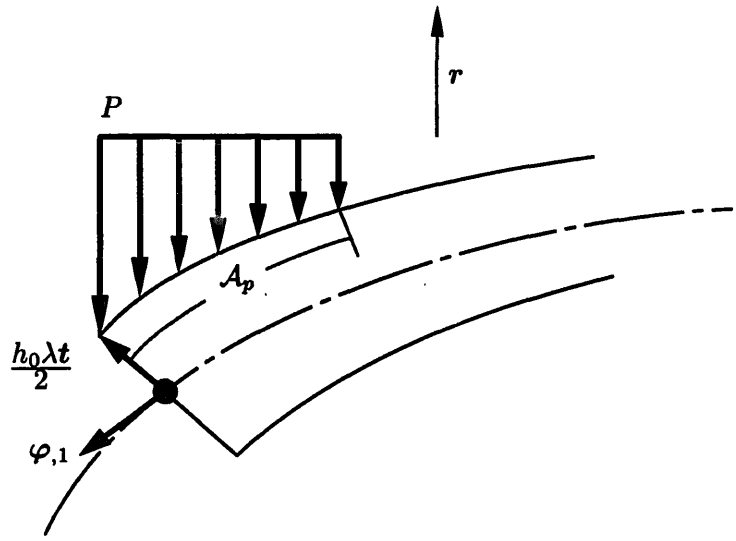

Fig. 3.2. Example of external surface loading on a shell-like body. The load P not only affects the mid-surface, but also the thickness stretch and director rotation variables.

As illustrated in Fig. 3.2, we consider a shell surface subjected to an external load $P(\xi^1, \xi^2)$[1] of fixed magnitude and orientation (i.e. dead loading) acting on some portion of the shell surface corresponding to the mid-surface section $\mathscr{A}_p$. Recall the definition of the external loading contribution to the weak form given by (2.14b)

$$G_{\text{ext}} := \int_{\mathscr{A}} [\bar{n} \cdot \delta\varphi + \bar{m} \cdot \delta d] \bar{j} \, d\xi^1 \, d\xi^2 + \int_{\partial\mathscr{A}} [n^\alpha \cdot \delta\varphi + \tilde{m}^\alpha \cdot \delta d] \nu_\alpha \bar{j} \, d\Gamma \,. \tag{3.10}$$

Having assumed zero body forces, the surface loading contribution becomes

$$G_{\text{ext}} = \int_{\mathscr{A}} \left[\frac{1}{\bar{j}} (j\sigma g^3) \Big|_{\xi=h^-}^{\xi=h^+} \cdot \delta\varphi + \frac{1}{\bar{j}} (\xi j \sigma g^3) \Big|_{\xi=h^-}^{\xi=h^+} \cdot \delta d \right] \bar{j} \, d\xi^1 \, d\xi^2 \,. \tag{3.11}$$

Neglecting terms of order h^2 and higher, the virtual work expression for the external loading can be written as

$$G_{\text{ext}} = \int_{\mathscr{A}} [P \cdot \delta\varphi + \tfrac{1}{2} P h_0 \cdot \delta d] \bar{j} \, d\xi^1 \, d\xi^2 \tag{3.12a}$$

$$=: \int_{\mathscr{A}_p} [P_\varphi \cdot \delta\varphi + P_\mu \, \delta\mu + P_t \cdot \delta t] \bar{j} \, d\xi^1 \, d\xi^2 \,, \tag{3.12b}$$

where $P_\varphi = P$, $P_\mu = \lambda h_0 P \cdot t/2$ and $P_t = \lambda h_0 P/2$ are the resulting mid-surface, thickness stretch and couple loading, respectively.

[1] Point loads can be easily accommodated by defining the external loading as a Dirac delta function, i.e., $P(\xi^1, \xi^2) = F \, \delta(\xi^1 - \bar{\xi}^1) \, \delta(\xi^2 - \bar{\xi}^2)$, where $(\bar{\xi}^1, \bar{\xi}^2)$ is the point of application.

REMARK 3.1. The linearization of the contribution of the external loading to the weak form (as given by (3.12a)) is non-zero. In fact, we have

$$\Delta G_{\text{ext}} = \int_{\mathscr{B}_p} \tfrac{1}{2} P h_0 \cdot \Delta(\delta d) \bar{j}\, d\xi^1\, d\xi^2 , \tag{3.13}$$

where $\Delta(\delta d) = \lambda\, \Delta\mu\, \delta t + \lambda\, \delta\mu\, \Delta t + \lambda\, \Delta\mu\, \delta\mu t - \lambda(\Delta t \cdot \delta t) t$. Neglecting this term will result in the loss of asymptotically quadratic rates of convergence for the Newton iteration solution procedure. This fact is illustrated numerically in Section 5.4.

3.4. *A simple elastic (isotropic) constitutive model*

To illustrate the significance of thickness stretching and its impact on the formulation of constitutive equations, we examine below the structure of the simplest possible elastic isotropic model. Thus, consider a complementary Gibbs free energy function of the following form:

$$\begin{aligned} \Psi^* = \frac{1}{2}\Big\{ & \frac{12}{Eh^3}\,[\nu A_{\alpha\beta}A_{\gamma\delta} - (1+\nu)A_{\alpha\delta}A_{\beta\gamma}]\check{m}^{(\alpha\beta)}\check{m}^{(\gamma\delta)} \\ & + \frac{2\nu}{Eh}\, A_{\alpha\beta}\check{n}^{\alpha\beta}\check{l}^3 - \frac{1}{Eh}\,(\check{l}^3)^2 - \frac{240(1+\nu)}{7Eh^3}\, A_{\alpha\beta}\check{m}^{3\alpha}\check{m}^{3\beta} \\ & + \frac{1}{Eh}\,[\nu A_{\alpha\beta}A_{\gamma\delta} - (1+\nu)A_{\alpha\delta}A_{\beta\gamma}]\check{n}^{\alpha\beta}\check{n}^{\gamma\delta} - \frac{1}{\kappa Gh}\, A_{\alpha\beta}\check{q}^{\alpha}\check{q}^{\beta}\Big\}, \end{aligned} \tag{3.14}$$

where $A_{\alpha\beta} = a^0_{\alpha\beta} = \varphi^0_{,\alpha} \cdot \varphi^0_{,\beta}$ are the covariant components of the reference mid-surface metric tensor. This expression may be obtained by an integration through the thickness of an assumed stress distribution in a manner described in [9]. Standard arguments then yield the following stress–strain relations:

$$\check{n}^{\alpha\beta} = \frac{Eh}{(1+\nu)\bar{J}}\left\{\left[\frac{\nu}{1-2\nu}\, A^{\alpha\beta}A^{\gamma\delta} + \frac{1}{2}\,(A^{\alpha\gamma}A^{\beta\delta} + A^{\alpha\delta}A^{\beta\gamma})\right]\varepsilon_{\gamma\delta} + \frac{\nu}{1-2\nu}\, A^{\alpha\beta}\chi\right\}, \tag{3.15a}$$

$$\check{l}^3 = \frac{Eh}{(1+\nu)(1-2\nu)\bar{J}}\,\{(1-\nu)\chi + \nu A^{\alpha\beta}\varepsilon_{\alpha\beta}\}, \tag{3.15b}$$

$$\check{q}^{\alpha} = \kappa\,\frac{Gh}{\bar{J}}\, A^{\alpha\beta}\delta_{\beta}, \tag{3.15c}$$

$$\check{m}^{\alpha\beta} = \frac{Eh^3}{12(1-\nu^2)\bar{J}}\left\{\nu A^{\alpha\beta}A^{\gamma\delta} + \frac{1-\nu}{2}\,(a^{\alpha\gamma}A^{\beta\delta} + A^{\alpha\delta}A^{\beta\gamma})\right\}\rho_{\gamma\delta}, \tag{3.15d}$$

$$\check{m}^{3\alpha} = \frac{7Eh^3}{240(1+\nu)\bar{J}}\, A^{\alpha\beta}\chi_{\beta}, \tag{3.15e}$$

where the strain measures in (3.15) are defined by (3.4).

REMARK 3.2. For the simple isotropic model (3.14), the matrix of (constant) elastic coefficients associated with the stress resultants $\{\check{n}^{\alpha\beta}, \check{q}^{\alpha}, \check{l}^{3}\}$ is identical to that arising in the linear isotropic three-dimensional theory.

REMARK 3.3. The plane stress assumption is not present in model (3.14). Nevertheless, as demonstrated in Section 5, plane stress response is automatically recovered in the thin shell limit. This conclusion follows at once by direct inspection of (3.15). Setting $\check{l}^{3}$ to zero and substituting the value of χ from (3.15b) into (3.15a), the plane stress constitutive matrix is obtained for the membrane stress components $\check{n}^{\alpha\beta}$.

REMARK 3.4. The preceding two remarks have a significant practical impact. Namely, in the context of the present formulation, which includes thickness stretch, the traditional plane stress assumption need not be enforced at the outset. As a result, the present formulation allows the implementation of three-dimensional models in a stress resultant form without resorting to the cumbersome reduction process required in the enforcement of the plane stress hypothesis; see e.g. [13, Chapter 6].

REMARK 3.5. From a numerical stand point, the essentially three-dimensional structure of the constitutive models requires the use of special interpolation techniques designed to circumvent the well-known difficulties with the incompressible limit; see e.g. [14]. In the present context, we employ an interpolation scheme constructed via a Hellinger–Reissner formulation for the membrane and thickness stretch fields, which is developed in Section 4 and evaluated numerically in Section 5.

REMARK 3.6. The through-the-thickness stress resultant $\check{l}^{3}$ is related linearly to the logarithmic stretch. We note that this constitutive model possesses the proper limits. As the thickness parameter λ goes to 0 or ∞, the energy goes to ∞. The numerical simulations below include an example (Section 5.4) of a thick shell problem where the overall membrane strains do not exceed 2%; however, due to localized effects of the surface loading, as much as 52% reduction in thickness is observed under the load. This example emphasizes the importance of constitutive models with stored energy functions possessing the correct asymptotic limit as the thickness goes to zero.

4. Interpolation; exact thickness updates

In this section, we examine the finite element implementation of the two formulations developed in the preceding section. We shall focus our analysis on the formulation presented in Section 3 which relies on the multiplicative decomposition of the director field into inextensible and stretching parts.

4.1. *Matrix formulation*; *mixed variational formulation*

For numerical analysis purposes, it proves convenient to arrange the stress resultants and couple components in vector form. To this end, we collect the mid-surface, director and

thickness stretch variations into component vectors (with the 3×2 transformation $\bar{\Lambda}$ defined in Part III)

$$\delta\varphi = \begin{bmatrix} \delta\varphi^1 \\ \delta\varphi^2 \\ \delta\varphi^3 \end{bmatrix}, \qquad \delta T = \begin{bmatrix} \delta T^1 \\ \delta T^2 \end{bmatrix}, \qquad \delta t = \bar{\Lambda}\, \delta T\,, \qquad \delta\Phi = \begin{bmatrix} \delta\varphi \\ \delta T \\ \delta\mu \end{bmatrix}. \tag{4.1}$$

The modified effective stress resultants are also written as component vectors, viz.,

$$\check{n} = \bar{J} \begin{bmatrix} \check{n}^{11} \\ \check{n}^{22} \\ \check{n}^{12} \end{bmatrix}, \qquad \check{q} = \bar{J} \begin{bmatrix} \check{q}^1 \\ \check{q}^2 \end{bmatrix}, \qquad \check{m} = \bar{J} \begin{bmatrix} \check{m}^{11} \\ \check{m}^{22} \\ \check{m}^{(12)} \end{bmatrix}, \qquad \check{l} = \bar{J} \begin{bmatrix} \check{m}^{31} \\ \check{m}^{32} \\ \check{l}^3 \end{bmatrix}, \tag{4.2}$$

where $\bar{J} = \bar{j}/\bar{j}_0$ is the mid-surface Jacobian of the deformation gradient. The (nonlinear) membrane, shear, bending and thickness stretch Lagrangian stain measures are given in matrix notation as

$$\varepsilon = \frac{1}{2} \begin{bmatrix} a_{11} - a_{11}^0 \\ a_{22} - a_{22}^0 \\ 2(a_{12} - a_{12}^0) \end{bmatrix}, \qquad \delta = \begin{bmatrix} \gamma_1 - \gamma_1^0 \\ \gamma_2 - \gamma_2^0 \end{bmatrix}, \qquad \rho = \begin{bmatrix} \kappa_{11} - \kappa_{11}^0 \\ \kappa_{22} - \kappa_{22}^0 \\ 2[\kappa_{(12)} - \kappa_{(12)}^0] \end{bmatrix},$$
$$\chi = \begin{bmatrix} \mu_1 - \mu_1^0 \\ \mu_2 - \mu_2^0 \\ \mu - \mu^0 \end{bmatrix}, \tag{4.3}$$

with the corresponding matrix differential operators

$$\mathbb{B}_m = \begin{bmatrix} \varphi^t_{,1} \dfrac{\partial}{\partial\xi_1} \\ \varphi^t_{,2} \dfrac{\partial}{\partial\xi^2} \\ \varphi^t_{,1} \dfrac{\partial}{\partial\xi^2} + \varphi^t_{,2} \dfrac{\partial}{\partial\xi^1} \end{bmatrix}_{3\times 3}, \qquad \mathbb{B}_{bm} = \begin{bmatrix} t^t_{,1} \dfrac{\partial}{\partial\xi_1} \\ t^t_{,2} \dfrac{\partial}{\partial\xi^2} \\ t^t_{,1} \dfrac{\partial}{\partial\xi^2} + t^t_{,2} \dfrac{\partial}{\partial\xi^1} \end{bmatrix}_{3\times 3},$$

$$\mathbb{B}_l = \begin{bmatrix} \dfrac{\partial}{\partial\xi^1} \\ \dfrac{\partial}{\partial\xi^2} \\ 1 \end{bmatrix}_{3\times 1}, \qquad \mathbb{B}_{sm} = \begin{bmatrix} t^t \dfrac{\partial}{\partial\xi^1} \\ t^t \dfrac{\partial}{\partial\xi^2} \end{bmatrix}_{2\times 3}, \tag{4.4}$$

$$\mathbb{B}_{sb} = \begin{bmatrix} \varphi^t_{,1} \\ \varphi^t_{,2} \end{bmatrix}_{2\times 3} \bar{\Lambda}_{3\times 2}, \qquad \mathbb{B}_{bb} = \mathbb{B}_m \bar{\Lambda}_{3\times 2}.$$

Introducing the notations

$$\mathbf{B}_{\text{total}} = \begin{bmatrix} \mathbb{B}_{\text{m}} & \mathbf{0} & \mathbf{0} \\ \mathbb{B}_{\text{sm}} & \mathbb{B}_{\text{sb}} & \mathbf{0} \\ \mathbb{B}_{\text{bm}} & \mathbb{B}_{\text{bb}} & \mathbf{0} \\ \mathbf{0} & \mathbf{0} & \mathbb{B}_{\text{l}} \end{bmatrix}_{11\times 6} \quad \text{and} \quad \check{r} = \begin{bmatrix} \check{n} \\ \check{q} \\ \check{m} \\ \check{l} \end{bmatrix}, \tag{4.5}$$

the weak form of the momentum balance equations may now be written as

$$G(\check{r}, \Phi, \delta\Phi) := \int_{\mathscr{A}} \check{r}^{\text{t}} \mathbb{B}_{\text{total}}\, \delta\Phi \bar{j}_0 \, \mathrm{d}\xi^1 \, \mathrm{d}\xi^2 - G_{\text{ext}}(\delta\Phi) . \tag{4.6}$$

REMARK 4.1. The added terms $\check{l}$, $\mathbb{B}_{\text{l}}$ and $\delta\mu$, which arise as a result of thickness stretch, are decoupled from the quantities defining the usual strain differential operators. As will be illustrated in Section 5, this feature is essential in order to maintain good numerical performance in the thin shell limit. The standard formulation (described in Section 4.4) avoids the use of the exponential map, at the expense of coupling the additional thickness terms to the total director increments. In the thin shell limit, this produces numerical ill-conditioning and locking response.

Following the developments in Parts II and III, the constitutive relations are enforced thorough a variational formulation which employs a Hellinger–Reissner functional for the membrane and thickness stretch fields and a Hu–Washizu functional for the transverse shear field. The remaining constitutive relations for the bending field and the added moments ($\check{m}^{3\alpha}$) may be enforced either via a Hellinger–Reissner functional or through a strong form (displacement formulation). The resulting functional takes the following form:

$$\Pi(\check{r}, \bar{\delta}, \Phi) = \Pi_{\text{m}}(\Phi, \check{n}, \check{l}^3) + \Pi_{\text{b}}(\Phi, \check{m}) + \Pi_3(\Phi, \check{m}^{3\alpha}) + \Pi_{\text{s}}(\Phi, \bar{\delta}, \check{q}) + \Pi_{\text{ext}}(\Phi) . \tag{4.7}$$

The functionals $\Pi_{\text{b}}(\Phi, \check{m})$ and $\Pi_{\text{s}}(\Phi, \bar{\delta}, \check{q})$ are identical to those from Part III and will not be discussed further. The term $\Pi_{\text{m}}(\Phi, \check{n}, \check{l}^3)$, on the other hand, is now defined by the expression

$$\Pi_{\text{m}}(\Phi, \check{n}, \check{l}^3) = \int_{\mathscr{A}} \begin{bmatrix} \check{n} \\ \bar{J}\check{l}^3 \end{bmatrix}^{\text{t}} \cdot \left(\begin{bmatrix} \varepsilon(\varphi) \\ \mu(\varphi) \end{bmatrix} - \frac{1}{2} C_m^{-1} \begin{bmatrix} \check{n} \\ \bar{J}\check{l}^3 \end{bmatrix} \right) \bar{j}_0 \, \mathrm{d}\xi^1 \, \mathrm{d}\xi^2 . \tag{4.8}$$

In particular, for the simple model developed in Section 3.4, the constitutive matrix C_{m}^{-1} takes the form (relative to an orthonormal basis constructed exactly as in Parts II and III)

$$C_{\text{m}}^{-1} := \frac{1}{Eh} \begin{bmatrix} 1 & -\nu & 0 & -\nu \\ -\nu & 1 & 0 & -\nu \\ 0 & 0 & 2(1+\nu) & 0 \\ -\nu & -\nu & 0 & 1 \end{bmatrix} . \tag{4.9}$$

In Part III of this work, the mixed interpolations for the membrane, shear and bending fields were described in the context of the inextensible director formulation. With the

exception of the membrane field, these interpolations remain the same for the present case and will therefore not be described in this section.

4.2. Membrane and thickness interpolations

The use of the mixed interpolation for the membrane field is essential since (as alluded to before) the constitutive equations take on a form similar to the equations of 3-dimensional elasticity which are well-known to cause severe locking in the incompressible limit. Within the context of the Hellinger–Reissner principle previously described, the residual and tangent stiffness contributions of the membrane and thickness resultants are constructed as follows.

1. Let $\bar{J}$ be the Jacobian transformation matrix at the center of the element in the reference configuration, and let $\bar{N}^I_{,a}$ be the Cartesian shape function derivatives at node I in the direction $\boldsymbol{n}_a$ (see e.g. Parts II and III of this work).

2. Assume the following distribution for the Cartesian components of the membrane and thickness resultants, discontinuous across elements,

$$\check{\boldsymbol{n}}_e = \boldsymbol{S}(\xi,\eta)\boldsymbol{\beta}_e = [\boldsymbol{1}_{4\times4}\|\boldsymbol{S}(\xi,\eta)]\boldsymbol{\beta}_e = \left[\begin{array}{c|c|c} \boldsymbol{1}_{4\times4} & \bar{\eta}\boldsymbol{f}_1\ \bar{\xi}\boldsymbol{f}_2 & \begin{matrix}\boldsymbol{0}_{3\times3}\\ \bar{\xi}\ \bar{\eta}\ \overline{\xi\eta}\end{matrix} \end{array}\right]\boldsymbol{\beta}_e, \tag{4.10}$$

where

$$\check{\boldsymbol{n}}_e := \begin{bmatrix} \check{n}^{11} \\ \check{n}^{22} \\ \check{n}^{12} \\ \check{l}^3 \end{bmatrix}, \quad \boldsymbol{f}_1 := \begin{bmatrix} \bar{J}^1_1\bar{J}^1_1 \\ \bar{J}^2_1\bar{J}^2_1 \\ \bar{J}^2_1\bar{J}^1_1 \\ 0 \end{bmatrix}, \quad \boldsymbol{f}_2 := \begin{bmatrix} \bar{J}^1_2\bar{J}^1_2 \\ \bar{J}^2_2\bar{J}^2_2 \\ \bar{J}^2_2\bar{J}^1_2 \\ 0 \end{bmatrix}, \tag{4.11}$$

$$\bar{\xi} := \xi - \frac{1}{\mathscr{A}_e}\int_{\mathscr{A}_e}\xi\,\mathrm{d}\mathscr{A}^0, \quad \bar{\eta} := \eta - \frac{1}{\mathscr{A}_e}\int_{\mathscr{A}_e}\eta\,\mathrm{d}\mathscr{A}^0, \quad \overline{\xi\eta} := \xi\eta - \frac{1}{\mathscr{A}_e}\int_{\mathscr{A}_e}\xi\eta\,\mathrm{d}\mathscr{A}^0, \tag{4.12}$$

with $\mathrm{d}\mathscr{A}^0 := \bar{j}_0\,\mathrm{d}\xi\,\mathrm{d}\eta$, and $\mathscr{A}_e := \int_{\mathscr{A}}\mathrm{d}\mathscr{A}^0$. The vector $\boldsymbol{\beta}_e \in \mathbb{R}^9$ contains the local element membrane stress resultant parameters.

3. Noting that $\int_{\mathscr{A}_e}\bar{\xi}\,\mathrm{d}\mathscr{A}^0 = \int_{\mathscr{A}_e}\bar{\eta}\,\mathrm{d}\mathscr{A}^0 = \int_{\mathscr{A}_e}\overline{\xi\eta}\,\mathrm{d}\mathscr{A}^0 = 0$, we have

$$\boldsymbol{H}_e := \int_{\mathscr{A}_e}\boldsymbol{S}^{\mathrm{t}}\boldsymbol{C}_{\mathrm{m}}^{-1}\boldsymbol{S}\,\mathrm{d}\mathscr{A}^0 = \begin{bmatrix} \mathscr{A}_e\boldsymbol{C}_{\mathrm{m}}^{-1} & \boldsymbol{0}_{4\times5} \\ \boldsymbol{0}_{5\times4} & \boldsymbol{h}_e \end{bmatrix}, \tag{4.13}$$

where

$$\boldsymbol{h}_e := \int_{\mathscr{A}_e}\boldsymbol{S}^{\mathrm{t}}\boldsymbol{C}_{\mathrm{m}}^{-1}\boldsymbol{S}\,\mathrm{d}\mathscr{A}^0. \tag{4.14}$$

Finally,

$$\boldsymbol{H}_e^{-1} = \begin{bmatrix} \dfrac{1}{\mathscr{A}_e}\boldsymbol{C}_m & \boldsymbol{0}_{4\times5} \\ \boldsymbol{0}_{5\times4} & \boldsymbol{h}_e^{-1} \end{bmatrix}, \tag{4.15}$$

where

$$\boldsymbol{C}_m := \frac{Eh}{(1+\nu)(1-2\nu)} \begin{bmatrix} 1-\nu & \nu & 0 & \nu \\ \nu & 1-\nu & 0 & \nu \\ 0 & 0 & \tfrac{1}{2}(1-2\nu) & 0 \\ \nu & \nu & 0 & 1-\nu \end{bmatrix}. \tag{4.16}$$

4. The discrete approximation to the linearized membrane strain–displacement operator at node I is defined as

$$\boldsymbol{B}_{\mathrm{m}}^I = \left[\begin{array}{c|c} \bar{N}^I_{,1}\boldsymbol{\varphi}_{,1} & 0 \\ \bar{N}^I_{,2}\boldsymbol{\varphi}_{,2} & 0 \\ \bar{N}^I_{,1}\boldsymbol{\varphi}_{,2} + \bar{N}^I_{,2}\boldsymbol{\varphi}_{,1} & 0 \\ \boldsymbol{0}_{1\times 3} & N^I \end{array}\right], \tag{4.17}$$

where

$$\boldsymbol{\varphi}_{,a} = \sum_{I=1}^{N_{\mathrm{en}}} \bar{N}^I_{,a}\boldsymbol{\varphi}_I\,, \quad a = 1,2\,. \tag{4.18}$$

5. The membrane and thickness stress resultants are computed in terms of the local stress parameters as

$$\check{\boldsymbol{n}}_e = \boldsymbol{S}^{\mathrm{t}}\boldsymbol{H}_{\mathrm{m}}^{-1}\boldsymbol{\beta}_e\,, \quad \text{where } \boldsymbol{\beta}_e = \int_{\mathscr{A}} \boldsymbol{S}_e^{\mathrm{t}}\boldsymbol{\varepsilon}_{\mathrm{m}}\,\mathrm{d}\mathscr{A}^0\,, \tag{4.19}$$

where the strains $\boldsymbol{\varepsilon}_{\mathrm{m}}$ are given by

$$\boldsymbol{\varepsilon}_{\mathrm{m}} := \frac{1}{2}\begin{bmatrix} \boldsymbol{\varphi}_{,1}\cdot\boldsymbol{\varphi}_{,1} - 1 \\ \boldsymbol{\varphi}_{,2}\cdot\boldsymbol{\varphi}_{,2} - 1 \\ 2\boldsymbol{\varphi}_{,1}\cdot\boldsymbol{\varphi}_{,2} \\ 2\chi \end{bmatrix}, \tag{4.20}$$

and the logarithmic thickness stretch μ is interpolated from the nodal values

$$\mu = \sum_{I=1}^{N_{\mathrm{en}}} \bar{N}^I\mu_I\,. \tag{4.21}$$

6. The contribution to the element material tangent stiffness associated with nodes I, J can be computed as

$$\boldsymbol{K}_{\mathrm{m}}^{IJ} = [\boldsymbol{G}^I]^{\mathrm{t}}\boldsymbol{H}_{\mathrm{m}}^{-1}\boldsymbol{G}^J\,, \tag{4.22}$$

where

$$\boldsymbol{G}^I := \int_{\mathscr{A}} \boldsymbol{S}^{\mathrm{t}}\boldsymbol{B}_{\mathrm{m}}^I\,\mathrm{d}\mathscr{A}^0\,. \tag{4.23}$$

The contribution to the geometric stiffness is

$$\boldsymbol{K}_{\mathrm{g}}^{IJ} = \check{n}^{ab}\bar{N}^I_{,a}\bar{N}^J_{,b}\boldsymbol{1}_{3\times 3}\,. \tag{4.24}$$

The c. .. ution to the residual load vector is

$$R^I = G^I \beta_e \,. \tag{4.25}$$

REMARK 4.2. The through-the-thickness stress resultant interpolation presented above was chosen to precisely recover the equivalent stress field that would result from a displacement formulation. In fact, the use of four stress parameters for the thickness resultant satisfies the condition that the number of stress parameters added to the number of rigid body modes of an element equals (or exceeds) its total number of degrees of freedom.

REMARK 4.3. The contributions of the added resultant stress couple $\check{m}^{3a}$ remain to be determined. For simplicity, we use a displacement formulation, where the discrete strain–displacement relations are

$$B^I_{\mathrm{m3}} = \begin{bmatrix} \bar{N}^I_{,1} \\ \bar{N}^I_{,2} \end{bmatrix}. \tag{4.26}$$

For the simple quadratic model in Section 3.4, the constitutive matrix relating $\{\check{m}^{3a}\}$ and $\{\chi_a\}$ is given by

$$C_{\mathrm{m3}} = \frac{7Eh^3}{240(1+\nu)} \begin{bmatrix} 1 & 0 \\ 0 & 1 \end{bmatrix}, \tag{4.27}$$

and the contribution to the tangent stiffness takes the form

$$K^{IJ}_{\mathrm{m3}} = \int_{\mathscr{A}} [B^I_{\mathrm{m3}}]^{\mathrm{t}} [C_{\mathrm{m3}}][B^J_{\mathrm{m3}}] \, \mathrm{d}\mathscr{A}^0 \,. \tag{4.28}$$

The logarithmic strains μ_a associated with χ_a, and stress resultants $\check{m}^{3a}$ are computed through the relations

$$\mu_a = \sum_{I=1}^{N_{\mathrm{en}}} \bar{N}^I_{,a} \mu_I \,, \qquad [\check{m}^{3a}] = [C_{\mathrm{m3}}][\chi_a] \,. \tag{4.29}$$

Finally, the residual contribution becomes

$$R^I_{\mathrm{m3}} = \int_{\mathscr{A}} [B^I_{\mathrm{m3}}]^{\mathrm{t}} \{\check{m}^{3a}\} \, \mathrm{d}\mathscr{A}^0 \,. \tag{4.30}$$

4.3. *Geometrically exact thickness update*

The construction of an update algorithm for the thickness stretch $\lambda : \mathscr{A} \to \mathbb{R}_+$ at the nodal points in the mid-surface of the shell is dictated by the following geometric considerations.

(i) At each point $x = \varphi(\xi^1, \xi^2)$ of the mid-surface, the thickness stretch $\lambda(\xi^1, \xi^2) > 0$ has the group property, since $\mathbb{R}_+$ is a group under multiplication, i.e.,

$$\lambda_1 \cdot \lambda_2 \in \mathbb{R}_+ \quad \text{for } \lambda_1, \lambda_2 \in \mathbb{R}_+ . \tag{4.31}$$

Thus, the composition of two stretches is by multiplication.

(ii) The Lie algebra associated with the group $\mathbb{R}_+$ is the entire real line $\mathbb{R}$ with addition as algebra operation. Thus, stretch increments are elements $\Delta\mu \in \mathbb{R}$ (positive or negative) composed by addition.

(iii) Elements in the Lie algebra $\mathbb{R}$ (incremental stretches) are mapped onto elements in the group $\mathbb{R}_+$ (stretches) via the exponential map $\exp: \mathbb{R} \to \mathbb{R}_+$. See Fig. 4.1 for a graphical illustration.

The preceding geometric considerations uniquely determine the correct update procedure for the thickness stretch as follows.

Let $\lambda^k \in \mathbb{R}_+$ be the stretch value in the k-iteration of the iterative solution procedure at a given (nodal) point $x = \varphi(\xi^1, \xi^2)$ of the mid-surface. Further, let $\Delta\mu^{k+1} \in \mathbb{R}$ be the incremental stretch at the point $x = \varphi(\xi^1, \xi^2)$ assumed to be given. The updated stretch at $x = \varphi(\xi^1, \xi^2)$ consistent with the geometric structure of the problem is then obtained by the standard formula

$$\lambda^{k+1} = \lambda^k \exp[\Delta\mu^{k+1}] . \tag{4.32}$$

Conceptually, this update is identical to the rotational updates developed in Parts I and III with the group SO(3) now replaced by the much simpler one-dimensional group $\mathbb{R}_+$.

In the present context, however, the preceding update takes a remarkably simple additive form which entirely avoids the use of the exponential map at each step of the iterative solution procedure. Recall that the shell theory of Section 3 is formulated entirely in terms of the logarithmic stretch $\mu := \ln \lambda$. Consequently, taking the logarithm of formula (4.32), we obtain the simple additive update procedure

$$\mu^{k+1} = \mu^k + \Delta\mu^{k+1} . \tag{4.33}$$

Thus, in terms of the logarithmic stretches, the update procedure is additive. The total finite stretch is then obtained once the calculation is completed by exponentiation as

$$\lambda_{\text{final}} = \exp[\mu_{\text{final}}] . \tag{4.34}$$

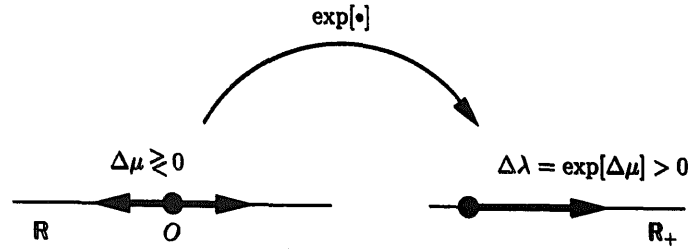

Fig. 4.1. The exponential map $\exp: \mathbb{R} \to \mathbb{R}_+$ mapping (positive or negative) incremental stretches $\Delta\mu \in \mathbb{R}$ into finite stretches $\lambda = \exp[\Delta\mu] > 0$.

As alluded to before, since the update of the inextensible part $t: \mathscr{A} \to S^2$ of the director field is identical to that considered in Part III, further details are omitted.

4.4. Standard one-director extensible shell model

The formulation described in the preceding section relies crucially on a multiplicative decomposition of the director field $d: \mathscr{A} \to \mathbb{R}^3$ into an inextensible part, defined by the unit vector field $t: \mathscr{A} \to S^2$, and a stretching part defined by the function $\lambda: \mathscr{A} \to \mathbb{R}_+$ (see Fig. 3.1).

Although this decomposition kinematically decouples the thickness stretch $\lambda(\xi^1, \xi^2) \in \mathbb{R}_+$ and the inextensible part $t(\xi^1, \xi^2) \in S^2$, these two fields remain coupled through the constitutive equations.

Alternatively, as discussed in Section 2, one may consider the formulation of the shell theory directly in terms of the director field $d: \mathscr{A} \to \mathbb{R}^3$, without explicitly introducing the preceding multiplicative decomposition at the outset. As pointed out above, the appeal of such an approach lies in the simple structure now taken by the configuration updates in an iterative solution procedure. In fact, in view of (2.4) and (2.12), the configurations and admissible variations now take values in the linear space $\mathbb{R}^3 \times \mathbb{R}^3$. Consequently, the update procedure becomes a simple addition. Namely: Let $\Phi^k = (\varphi^k, d^k) \in \mathscr{C}$ be given and let $\Delta\Phi^{k+1} = (\Delta\varphi^{k+1}, \Delta d^{k+1}) \in T_{\Phi^k}\mathscr{C}$ be a given configuration increment. The updated configuration $\Phi^{k+1} = (\varphi^{k+1}, d^{k+1}) \in \mathscr{C}$ is then obtained by the simple expressions

$$\varphi^{k+1} = \varphi^k + \Delta\varphi^{k+1} \tag{4.35a}$$

$$d^{k+1} = d^k + \Delta d^{k+1}. \tag{4.35b}$$

Further insight into the updates associated with this formulation and the approach presented in the preceding section can be gained by examining Fig. 4.2, where the relationship between these two updates is illustrated in the inextensible limit $\lambda \to 1$. Formulae (4.35) can be interpreted as a secant update of the inextensible director field enforced essentially by a penalty method. In Section 5, we illustrate numerically the fact that the simple update formula (4.35b) becomes progressively ill-conditioned in the thin-shell limit; as expected from classical results on penalty methods; see e.g. [15].

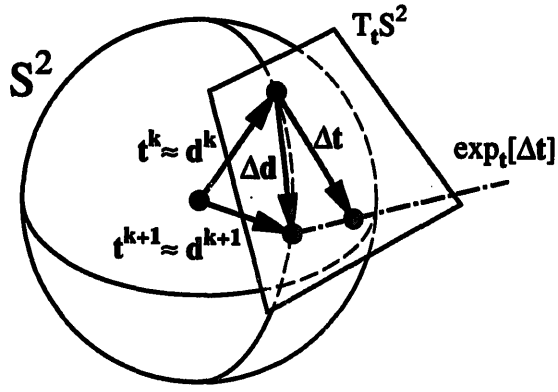

Fig. 4.2. Relationship between the director updates in the thin shell limit ($\lambda \to 1$) for the standard extensible director formulation and the inextensible director formulation of Part III.

Despite the shortcomings alluded to before, the standard director formulation leads to a very attractive computational framework. Thus, we conclude this section with an outline of the matrix formulation for the standard extensible director formulation. The weak form of the equilibrium equations given for the present formulation by (2.17) can be expressed in matrix notation as follows. Set

$$\tilde{\mathbb{B}}_{bm} = \begin{bmatrix} \boldsymbol{d}^t_{,1} \dfrac{\partial}{\partial \xi^1} \\ \boldsymbol{d}^t_{,2} \dfrac{\partial}{\partial \xi^2} \\ \boldsymbol{d}^t_{,1} \dfrac{\partial}{\partial \xi^2} + \boldsymbol{d}^t_{,2} \dfrac{\partial}{\partial \xi^1} \end{bmatrix}_{3\times 3}, \qquad \tilde{\mathbb{B}}_l = \begin{bmatrix} \boldsymbol{d}^t_{,1} + \boldsymbol{d}^t \dfrac{\partial}{\partial \xi^2} \\ \boldsymbol{d}^t_{,2} + \boldsymbol{d}^t \dfrac{\partial}{\partial \xi^2} \\ \boldsymbol{d}^t \end{bmatrix}_{3\times 3}, \tag{4.36a}$$

$$\tilde{\mathbb{B}}_{sm} = \begin{bmatrix} \boldsymbol{d}^t \dfrac{\partial}{\partial \xi^1} \\ \boldsymbol{d}^t \dfrac{\partial}{\partial \xi^2} \end{bmatrix}_{2\times 3}, \qquad \tilde{\mathbb{B}}_{sb} = \begin{bmatrix} \boldsymbol{\varphi}^t_{,1} \\ \boldsymbol{\varphi}^t_{,2} \end{bmatrix}_{2\times 3}. \tag{4.36b}$$

The weak form (2.17) then takes the form

$$\begin{aligned} G(\boldsymbol{\Phi}, \delta\boldsymbol{\Phi}) = \int_{\mathscr{A}} \Big[(\mathbb{B}_m \delta\boldsymbol{\varphi}) \cdot \tilde{\boldsymbol{n}} + \left([\tilde{\mathbb{B}}_{sm} \tilde{\mathbb{B}}_{sb}] \begin{bmatrix} \delta\boldsymbol{\varphi} \\ \delta\boldsymbol{d} \end{bmatrix} \right) \cdot \tilde{\boldsymbol{q}} \\ + \left([\tilde{\mathbb{B}}_{bm} \mathbb{B}_m] \begin{bmatrix} \delta\boldsymbol{\varphi} \\ \delta\boldsymbol{d} \end{bmatrix} \right) \cdot \tilde{\boldsymbol{m}} + (\tilde{\mathbb{B}}_l \delta\boldsymbol{d}) \cdot \tilde{\boldsymbol{l}} \Big] \bar{j}_0 \, d\xi^1 \, d\xi^2 - G_{ext}(\delta\boldsymbol{\Phi}) \\ = \int_{\mathscr{A}} \left(\tilde{\mathbb{B}}_{total} \begin{bmatrix} \delta\boldsymbol{\varphi} \\ \delta\boldsymbol{d} \end{bmatrix} \right) \cdot \tilde{\boldsymbol{r}} \, \bar{j}_0 \, d\xi^1 \, d\xi^2 - G_{ext}(\delta\boldsymbol{\Phi}), \end{aligned} \tag{4.37a}$$

where the stress and stress couple vectors are given by

$$\tilde{\boldsymbol{n}} = \bar{J} \begin{bmatrix} \tilde{n}^{11} \\ \tilde{n}^{22} \\ \tilde{n}^{12} \end{bmatrix}, \quad \tilde{\boldsymbol{q}} = \bar{J} \begin{bmatrix} \tilde{q}^1 \\ \tilde{q}^2 \end{bmatrix}, \quad \tilde{\boldsymbol{m}} = \bar{J} \begin{bmatrix} \tilde{m}^{11} \\ \tilde{m}^{22} \\ \tilde{m}^{(12)} \end{bmatrix}, \quad \tilde{\boldsymbol{l}} = \bar{J} \begin{bmatrix} \tilde{m}^{31} \\ \tilde{m}^{32} \\ \tilde{l}^3 \end{bmatrix}, \tag{4.37b}$$

and

$$\tilde{\mathbb{B}}_{total} = \begin{bmatrix} \mathbb{B}_m & \mathbf{0} \\ \tilde{\mathbb{B}}_{sm} & \tilde{\mathbb{B}}_{sb} \\ \tilde{\mathbb{B}}_{bm} & \mathbb{B}_m \\ \mathbf{0} & \tilde{\mathbb{B}}_l \end{bmatrix}_{11\times 6} \quad \text{and} \quad \tilde{\boldsymbol{r}} = \begin{bmatrix} \tilde{\boldsymbol{n}} \\ \tilde{\boldsymbol{q}} \\ \tilde{\boldsymbol{m}} \\ \tilde{\boldsymbol{l}} \end{bmatrix}. \tag{4.37c}$$

Using the preceding matrix notation, the linearization of the strain measures (2.16) at $\boldsymbol{\Phi}$ can be expressed as

$$\begin{bmatrix} \delta\boldsymbol{\varepsilon} \\ \delta\tilde{\boldsymbol{\gamma}} \\ \delta\tilde{\boldsymbol{\rho}} \\ \delta\tilde{\boldsymbol{\chi}} \end{bmatrix} := \frac{d}{d\varepsilon}\Big|_{\varepsilon=0} \begin{bmatrix} \boldsymbol{\varepsilon}(\boldsymbol{\Phi}_\varepsilon) \\ \tilde{\boldsymbol{\gamma}}(\boldsymbol{\Phi}_\varepsilon) \\ \tilde{\boldsymbol{\rho}}(\boldsymbol{\Phi}_\varepsilon) \\ \tilde{\boldsymbol{\chi}}(\boldsymbol{\Phi}_\varepsilon) \end{bmatrix} = \tilde{\mathbb{B}}_{total} \begin{bmatrix} \delta\boldsymbol{\varphi} \\ \delta\boldsymbol{d} \end{bmatrix}, \tag{4.38}$$

where

$$\Phi_\varepsilon = (\varphi + \varepsilon\delta\varphi, d + \varepsilon\delta d) \in \mathscr{C}, \quad \varepsilon > 0, \tag{4.39}$$

for $(\delta\varphi, \delta d) \in \mathscr{C}$.

Finally, for simplicity, we restrict our attention to elastic constitutive equations with identical structures as in Section 2.4 but now formulated in terms of the effective stress resultants and conjugate strain measures developed in this section.

The finite element implementation of the alternative formulation obtained above is constrained from the isoparametric interpolations

$$\varphi|_{\mathscr{A}_e} = \sum_{A=1}^{N_{en}} N^A(\xi,\eta)\varphi_A, \quad d|_{\mathscr{A}_e} = \sum_{A=1}^{N_{en}} N^A(\xi,\eta)d_A, \tag{4.40}$$

along with the mixed finite element approximations for membrane, bending and transverse shear strains, essentially identical to those given in Section 3 and Part III. As mentioned before, in the present context, the configuration update procedure has the simple additive structure given by (4.35). Details pertaining to the assumed transverse shear strain field and the linearization of the weak form (4.37) are fairly straightforward and are presented in Appendices A and B. Numerical simulations employing the resulting finite element formulation which illustrate the ill-conditioning of the method in the thin shell limit are presented in the following section. In spite of these numerical difficulties, its inherent simplicity makes the present formulation very attractive from a computational standpoint. As in the penalty formulation of incompressibility constraint in elasticity, we believe that a judicious choice of numerical analysis techniques (e.g., the method of augmented Lagrangians, see [16]) may ultimately produce a very effective computational strategy. In its present form, however, this methodology is not competitive with the procedure discussed in Sections 2 and 3.

5. Numerical simulations

In the following sections, we present numerical simulations to demonstrate the following important issues:

(i) For thin shells, the multiplicative formulation reduces to that of the inextensible director formulation with no numerical ill-conditioning;

(ii) In contrast to the multiplicative formulation, the formulation based on the standard single extensible director exhibits ill-conditioning in the thin limit and, therefore, is suitable only for the analysis of thick shells;

(iii) As noted previously, the constitutive relations which incorporate thickness stretch resemble those from three-dimensional elasticity, which are known to cause severe locking with the displacement formulation in the incompressible limit. The proposed mixed interpolation alleviates this locking behavior exhibited by the displacement formulation;

(iv) The proper application of external surface loading is crucial for capturing localized thickness change effects for moderately thick and thick shell problems;

(v) Asymptotically quadratic rates of convergence are obtained for the Newton iteration solution procedure.

Our present implementation uses the Hellinger–Reissner mixed interpolation for the

membrane and thickness resultants, the Hu–Washizu formulation (described in Part III) for the shear interpolation, and the standard displacement formulation for the bending resultants (also described in Part III).

5.1. *Thin-shell limit, linear benchmarks*

In this section, we examine the performance of the formulations described above in a number of selected examples for thin shell problems usually used as benchmarks for the linear theory. The results of the inextensible director formulation for the following and several other problems were presented in Part II. The results of this section demonstrate that in the thin shell limit, the solutions of the multiplicative formulation are identical to those of the inextensible director formulation. Furthermore, no ill-conditioning of the present formulation for this class of problem is observed. The formulation based on the standard extensible director theory, on the other hand, exhibits poor behavior in the thin shell limit and locks for coarse meshes.

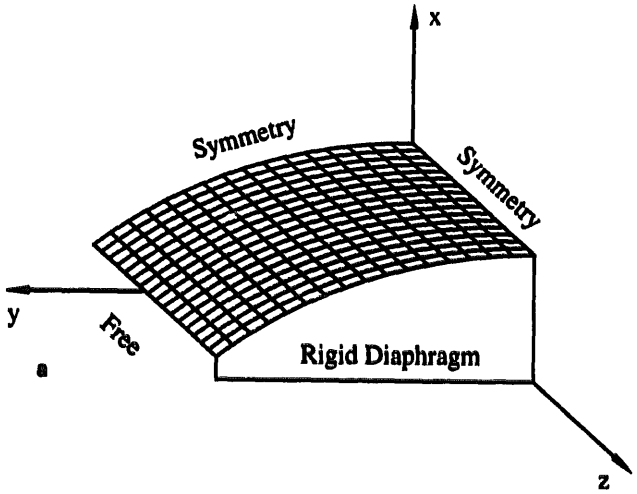

Fig. 5.1(a). The Scordellis–Lo barrel vault problem: a cylindrical panel supported by two end rigid diaphragms and subjected to gravity loading in the x direction. Two meshes are used to discretize a quarter-section of the problem, employing symmetry boundary conditions.

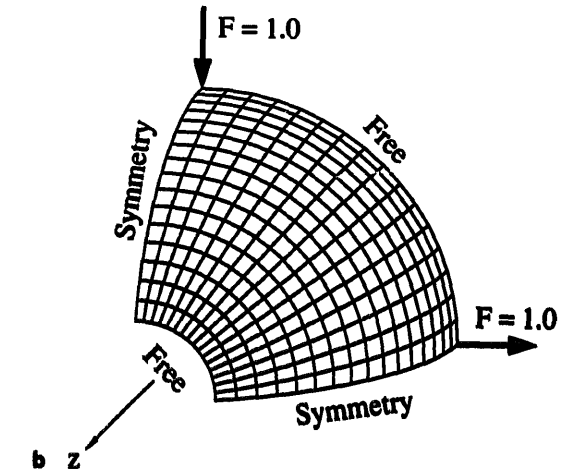

Fig. 5.1(b). The pinched hemisphere problem (with 180° hole): a hemisphere with two pairs of inward and outward forces, acting 90° apart. Three meshes are used to discretize a quarter-section of the problem, employing symmetry boundary conditions.

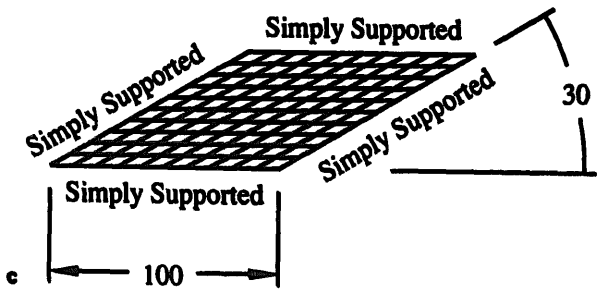

Fig. 5.1(c). The rhombic plate problem: a flat plate in the shape of a 30° rhombus, is simply supported on all four edges, and subjected to pressure loading. Two meshes are used to discretize the problem, employing simply supported ($w = 0$) boundary conditions.

5.1.1. Scordellis–Lo barrel vault

The Scordellis–Lo barrel vault, a short cylindrical section loaded by gravity, is a membrane dominated problem involving complex states of membrane stresses. The length of the cylinder is $L = 50$, the radius is $R = 25$, the thickness is $t = 0.25$, and the span angle of the section is $\phi = 80°$ (Fig. 5.1(a)). The material properties are $E = 4.32 \times 10^7$ and $\nu = 0$. The solution to this problem was obtained numerically by Scordellis and Lo [17]. The authors report a value of 0.3024 for the displacement at the center of the panel. The results for two mesh configurations are listed in Table 5.1.

5.1.2. Pinched hemisphere (with 18° hole)

A pinched hemispherical shell with two inward and two outward forces 90° apart is modeled using symmetry boundary conditions on one quadrant (Fig. 5.1(b)). This problem is a good test problem used to assess the ability of a finite element method to capture inextensional bending behavior and to model rigid body modes. The material properties for this problem are $E = 6.825 \times 10^7$ and $\nu = 0.3$, with radius $R = 10$ and thickness $h = 0.04$. The results for the displacements under the load for three mesh configurations are listed in Table 5.2.

5.1.3. Bending of a thin rhombic plate

A simply-supported rhombic plate of side $l = 100$, material properties $E = 10 \times 10^6$, $\nu = 0.3$ and thickness $h = 1.0$ is uniformly loaded by pressure (Fig. 5.1(c)). The center-point deflection is compared to the analytical solution of 0.04455 obtained by Morely [18, 19]. The results for two mesh configurations are listed in Table 5.3.

Table 5.1
Scordellis–Lo barrel vault. Displacement at the center of the panel

Mesh configuration	Inextensible formulation	Multiplicative formulation	Standard formulation
4 × 4	0.31608	0.31608	0.31194
8 × 8	0.30384	0.30384	0.30352

Table 5.2
Pinched hemisphere. Displacement under pinching loads

Mesh configuration	Inextensible formulation	Multiplicative formulation	Standard formulation
4 × 4	0.092530	0.092530	0.008726
8 × 8	0.092697	0.092696	0.080216
16 × 16	0.092990	0.092990	0.092581

Table 5.3
Rhombic plate. Central plate deflection

Mesh configuration	Inextensible formulation	Multiplicative formulation	Standard formulation
8 × 8	0.038523	0.038523	0.038523
16 × 16	0.041174	0.041174	0.041174

REMARK 5.1. One observes that the results of the preceding sections are virtually identical for the inextensible director and the multiplicative formulations. The formulation based on the standard extensible director theory, on the other hand, locks for problems involving initial curvature in the thin shell limit. For initially flat problems, the latter approach coincides with the multiplicative formulation only in the linear theory. For non-linear problems involving large deformations, the two formulations produce very different results as shown below.

5.2. Thin-shell limit; large deformations

It can be seen that the formulation based directly on the standard extensible director theory, discussed in Section 4.4, lends itself to less complex implementation than the multiplicative formulation, and hence may seem more attractive for large scale computations. Unfortunately, as already pointed out, the former approach suffers from numerical ill-conditioning in the thin-shell limit and can only be recommended for the analysis of thick shells. This numerical ill-conditioning is manifested in both the convergence of the Newton iterations and the integrity of the solutions for thin shells. This behavior is demonstrated in two examples. These examples illustrate an increase in the computational effort and locking in the solutions for thin shells. In contrast, the multiplicative formulation maintains its excellent performance and produces results identical to those from the inextensible formulation in the thin shell limit.

5.2.1. Thin beam bending

A beam of length $L = 10$ and width $w = 1$ is clamped on one end, and subjected to two point loads acting on the mid-surface of the free end (Fig. 5.2). Three different values are used for the thickness of the beam: $h = 1, 0.1, 0.01$, to produce length to thickness ratios of 10, 100 and 1000. A 10 element mesh is used to model this problem, with material properties $E = 10 \times 10^6$, $\nu = 0.3$. The results for the inextensible theory in Part III are compared with the results obtained with the multiplicative formulation and the formulation based on the standard extensible director theory in Table 5.4 for a load of $F = 100\,000 \times h^3$. The results in Table 5.4 show clearly that the multiplicative formulation reduces to the inextensible theory of Part III in the thin shell limit without loss of accuracy or efficiency. This is not the case for the standard extensible director approach, which reproduces good results for the thick shell case ($L/h = 10$), but deteriorates rapidly for thin beams, with severe loss of accuracy and increased computational cost due to numerical ill-conditioning. A tolerance of 10^{-20} is employed in the Newton iteration scheme for each of the problems (i.e., the solution is considered converged

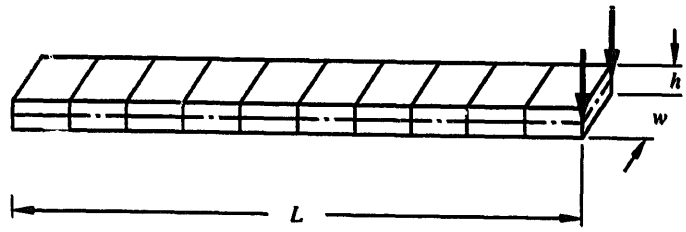

Fig. 5.2. Problem definition and mesh discretization of the large deformation beam bending problem.

Table 5.4
Thin beam bending. $FL^3/Ewh^3 = 100$. Tip deflection under point load (using 5 load steps)

L/h Ratio	10	100	1000
	Vertical displacement		
Multiplicative	7.3839	7.3061	7.3053
Standard	7.3535	7.0848	5.7924
Inextensible	7.3849	7.3061	7.3053
	Horizontal displacement		
Multiplicative	4.1616	4.1173	4.1168
Standard	4.1144	3.8992	2.6362
Inextensible	4.1630	4.1173	4.1168
	Number of iterations. First step		
Multiplicative	7	10	12
Standard	7	11	26
Inextensible	7	10	12
	Number of iterations. Total		
Multiplicative	33	48	61
Standard	35	54	88
Inextensible	33	48	61

when the energy norm is reduced by a factor of at least 10^{-20} compared to the first iteration of a given time step).

5.2.2. *Pinched hemisphere: large deformation version*

The pinched hemisphere problem of Section 5.1.2 is extended to the finite deformation regime to examine, once more, a comparative performance of the multiplicative formulation, the formulation based on the standard extensible director, and the inextensible director model in Part III (which should be recovered in the thin limit). The thickness chosen for this case is $h = 0.01$ yielding a radius to thickness ratio of $R/h = 1000$. This problem was analyzed using 12 load steps, to yield a final displacement of approximately half of the initial radius of the sphere. The load–deflection results are plotted in Fig. 5.3 for all formulations along with the final deformed configuration of the sphere.

The thin-shell behavior of the previous problem is observed again in the present problem. The multiplicative approach recovers the results of the classical inextensible director model, while the formulation based on the standard extensible director theory exhibits locking due to numerical ill-conditioning. Using a tolerance of 10^{-20}, a total of 105 Newton iterations were used in computing the solution for both the classical inextensible and the multiplicative formulations, while 115 iterations were required for the formulation based on the standard extensible director theory.

5.3. *Incompressible limit*

As noted previously, the constitutive relations, which account for thickness change, take on the form of the full three-dimensional equations without resorting to the plane stress

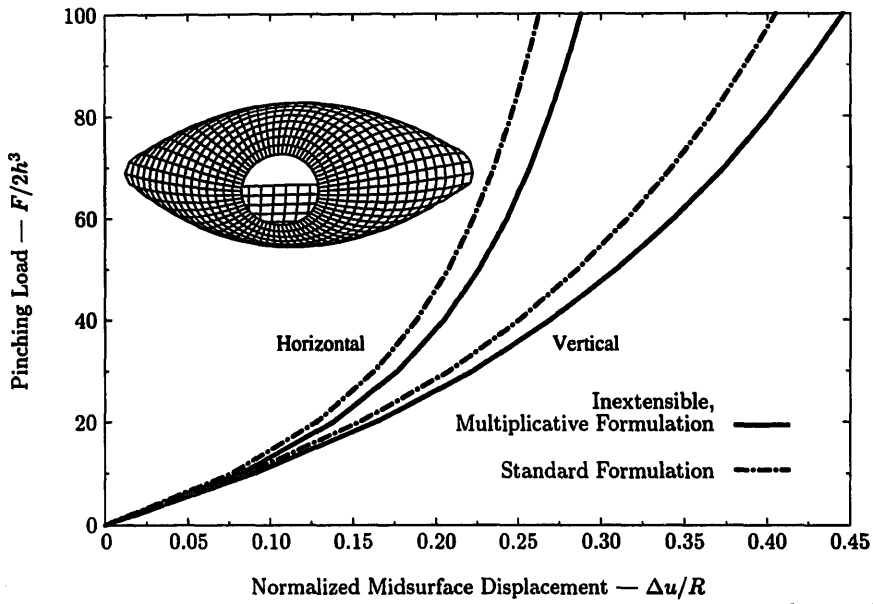

Fig. 5.3. Load–deflection plots of the large deformation, pinched hemisphere problem. The load for the inextensible director model in Part III, the multiplicative formulation in Section 3, and the formulation in Section 4.4 based on the standard extensible director theory are plotted against the deflections under the vertical and horizontal point loads. The inset depicts the final deformed configuration.

assumption. It is well-known that these constitutive relations exhibit severe locking of the displacement formulation in the incompressibility limit. In this section, we give an example of this parasitic behavior and demonstrate the ability of the proposed mixed finite element method to alleviate this phenomenon.

A beam of length $L = 10$ and height $h = 2$ is clamped on one edge and subjected to an in-plane bending moment at the other (see Fig. 5.4). The Young's modulus is $E = 4 \times 10^3$ and three different values of the Poisson's ratio are used: $\nu = 0$, 0.25, 0.49999. The beam is modeled with a 10×4 finite element mesh. This problem is examined for two different cases: plane strain, modeled by simply constaining all thickness stretch degrees of freedom to be zero as a boundary condition, and thickness stretch, where no constraint on the thickness degree of freedom is used. The results of this linear problem are listed in Table 5.5.

Table 5.5
Incompressible beam binding. Deflection at center due to bending moment

ν	Displacement	Mixed	Exact
0.00	0.18330	0.20623	0.20625
	Plain strain		
0.25	0.17545	0.19329	0.19336
0.49999	0.00020	0.15455	0.15469
	Thickness stretch		
0.25	0.18592	0.20400	
0.49999	0.13978	0.19667	

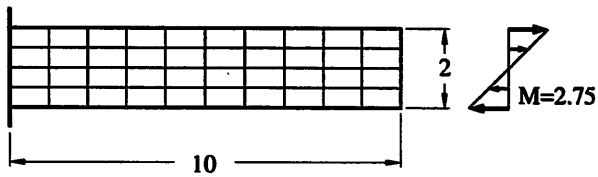

Fig. 5.4. Clamped, nearly incompressible, in-plane beam bending problem. The beam is modeled with a 10×4 finite element mesh.

It can be seen that the mixed method performs very well for all cases, including the incompressible limit, while the displacement formulation lags behind for small values of ν and locks severely for the nearly incompressible limit in plane strain.

REMARK 5.2. The displacement formulation solutions to the nearly incompressible problem are reasonable only for the case where thickness stretch is allowed. For the plane strain case, however, this formulation produces nearly zero displacement. This indicates that for problems where the thickness stretch may be constrained (e.g., contact or external surface loading) severe locking will occur, producing suspect numerical results. Furthermore, the mixed formulation exhibits superior coarse mesh accuracy behavior and is less sensitive to mesh distortion (see Parts II and III). Therefore, we regard the pure displacement formulation for the membrane fields unacceptable in the incompressible limit and the mixed formulation to be of critical importance.

5.4. *Large deformations, illustrative example*

The collapse of a clamped hemispherical shell of a rubber material (racket ball), introduced in [24], was analyzed in Part III using the inextensible director assumption. The hemisphere (radius $R = 26.3$ mm, and thickness $t = 4.4$ mm) is clamped along the circumference and subjected to a point load at the pole. This problem is used to demonstrate the localized effects of thickness change and the importance of the correct surface loading.

The material properties for this problem are $E = 4000$ kPa and $\nu = 0.4999$. The spherical shell (Fig. 5.5(a)) is analyzed using one quadrant, symmetry boundary conditions and a 16×16 finite element mesh. Load control was used to drive the top of the hemisphere the distance of the radius (complete collapse) in 10 steps. The multiplicative formulation is used to analyze this problem with the incorrect mid-surface loading and the correct top-surface loading (which results in loading of the thickness change variable).

Figure 5.5(b) plots the degree of thickness change against the displacement of the mid-surface for the correct and incorrect loading. The incorrect loading produces almost no thickness change—only about 1% under the load. The correct loading, however, exhibits the anticipated localized effects. The thickness changes by more than 50% under the load.

The load–deflection plots for the inextensible formulation of Part III and the results for the multiplicative formulation with the correct loading term are presented in Fig. 5.5(c). The load–deflection results for both situations coincide when plotted against the mid-surface displacement. However, when the load is plotted against the top-surface displacement (i.e., the true point of application of the load), a significant change is observed for the correct loading. This result emphasizes the importance of localized thickness change effects.

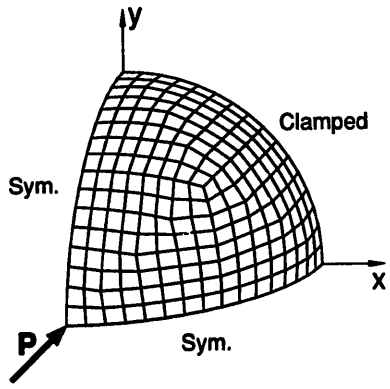

E = 4000.0 kPa
ν = 0.4999
Mesh = 16 x 16
R = 26.3 mm
t = 4.4 mm

Fig. 5.5(a). Problem definition of the collapse of a rubber sphere. A quarter-section of the hemisphere is discretized and symmetry conditions are used.

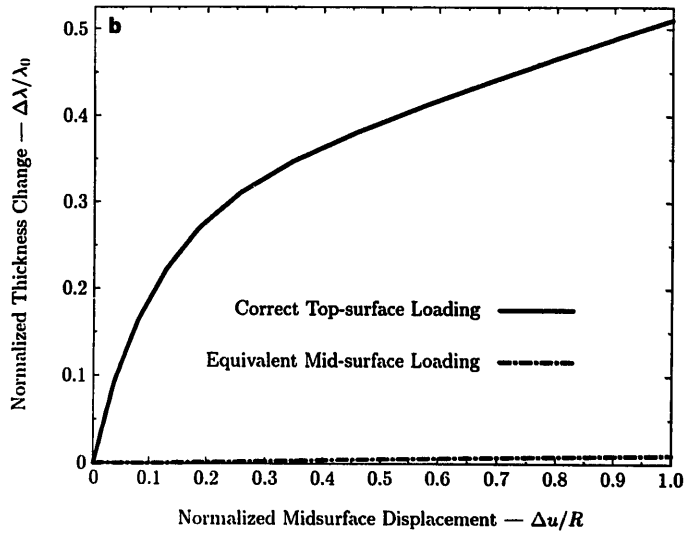

Fig. 5.5(b). The change in thickness of the point under the load plotted against the mid-surface displacement of the extensible formulation using both the correct top-surface and incorrect mid-surface loading. The correct loading results in ≈52% change at final collapse.

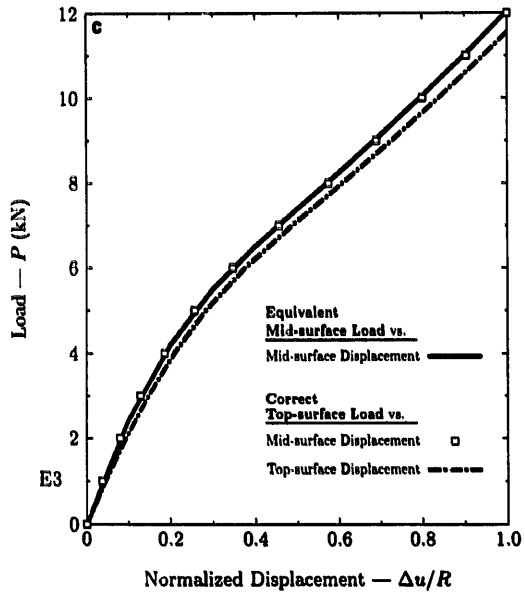

Fig. 5.5(c). The load–deflection curves obtained with the inextensible director model of Part III and multiplicative formulation, using the correct top-surface loading and incorrect mid-surface loading.

We present one final illustration of the localized thickness change effect. The final deformed configuration using the incorrect loading is shown in Fig. 5.6(a), whereas Fig. 5.6(b) shows the deformed configuration when the correct loading is employed. The former case produces almost no thickness change, whereas the latter yields the anticipated change in thickness localized to the point of application of the load. The deformation produced by the correct loading appears physically more reasonable.

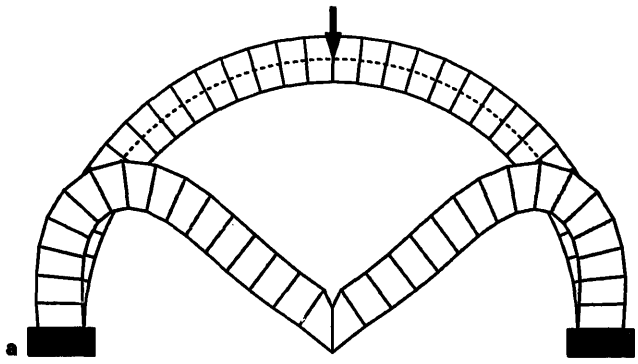

Fig. 5.6(a). Sectional view of the final configuration of the sphere subject to the incorrect equivalent mid-surface load. Virtually no thickness change is produced even under the load. The localized effect of the point load that is produced is transmitted to the top-, bottom- and mid-surfaces alike. The bottom-surface exhibits a 'kink' under the point load, which is only expected for thin shells.

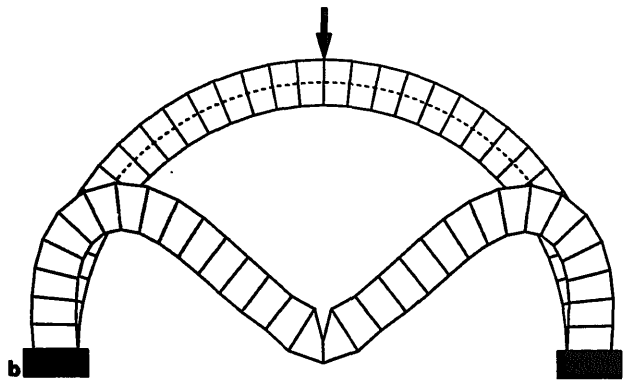

Fig. 5.6(b). Sectional view of the final configuration of the sphere subject to the correct top-surface load. A thickness change of approximately 52% is exhibited under the point load. The effects of that load are now localized to the top-surface only. The bottom-surface no longer exhibits the 'kink' and regains the smoothness expected in thick shells.

5.5. *Convergence results for the Newton iterations*

Since the exact closed-form expression for the tangent stiffness is available, standard Newton iterations converge at asymptotically quadratic rates. We present in Table 5.6(a) the results of the Newton iterations for the first load step in the collapse of a rubber sphere. In order to emphasize the importance of the linearization of the loading term, Table 5.6(a) contains the convergence results of the multiplicative formulation with and without the loading contribution to the geometric part of the tangent stiffness. It is readily apparent that the quadratic rate of convergence is present only when the correct linearization is used. The incomplete linearization exhibits an asymptotically linear rate of convergence and requires 5 additional iterations to obtain the desired tolerance (10^{-20}). In addition, Table 5.6(b) depicts the convergence rates of the multiplicative and standard formulations in the beam bending problem of Section 5.2.1 for the first load step for the case $L/h = 1000$ (thin-shell limit). The ill-conditioning of the latter formulation results in more than double the number of iterations to obtain convergence. Nevertheless, asymptotically quadratic rates of convergence are obtained in both formulations due to the presence of the exact linearization in the tangent stiffness.

6. Concluding remarks

In this paper, we have extended the geometrically exact shell theory and finite element implementation of Parts I, II and III to include the important effects of thickness stretch and initial variable thickness. We have examined in detail two possible approaches: (1) a formulation directly based on the standard single extensible director model, and (2) an alternative approach based on a multiplicative decomposition of the extensible director into a unit vector and a (positive) stretch. We have shown that the first approach circumvents the need for rotational updates but leads to numerical ill-conditioning in the thin shell limit. On

Table 5.6
Convergence in energy norms. First load step. True Newton–Kantorovitch iterations of Sections 5.3 and 5.2.1.

	(a) Section 5.3 Collapse of a rubber sphere		(b) Section 5.2.1 Thin beam bending ($L/h = 1000$)	
Iteration number	Incomplete tangent	Complete tangent	Multiplicative formulation	Standard formulation
0	$0.114 \times 10^{+04}$	$0.111 \times 10^{+04}$	0.363×10^{-01}	0.363×10^{-01}
1	$0.116 \times 10^{+05}$	$0.117 \times 10^{+05}$	$0.112 \times 10^{+05}$	$0.313 \times 10^{+05}$
2	$0.133 \times 10^{+02}$	$0.919 \times 10^{+01}$	$0.227 \times 10^{+03}$	$0.592 \times 10^{+03}$
3	$0.716 \times 10^{+00}$	$0.534 \times 10^{+00}$	$0.232 \times 10^{+00}$	$0.430 \times 10^{+00}$
4	0.546×10^{-03}	0.622×10^{-04}	0.399×10^{-04}	0.845×10^{-02}
5	0.469×10^{-05}	0.160×10^{-09}	0.284×10^{-03}	0.323×10^{-02}
6	0.528×10^{-07}	0.119×10^{-19}	0.187×10^{-04}	0.707×10^{-01}
7	0.594×10^{-09}	—	0.693×10^{-03}	0.220×10^{-02}
8	0.668×10^{-11}	—	0.190×10^{-05}	0.709×10^{-01}
9	0.751×10^{-13}	—	0.240×10^{-04}	0.195×10^{-03}
10	0.844×10^{-15}	—	0.124×10^{-09}	0.549×10^{-02}
11	0.951×10^{-17}	—	0.111×10^{-12}	0.159×10^{-03}
12	—	—	0.240×10^{-22}	0.952×10^{-02}
13	—	—	—	0.397×10^{-03}
14	—	—	—	$0.889 \times 10^{+00}$
15	—	—	—	0.935×10^{-05}
16	—	—	—	0.118×10^{-04}
17	—	—	—	0.135×10^{-04}
18	—	—	—	0.165×10^{-03}
19	—	—	—	0.245×10^{-04}
20	—	—	—	0.695×10^{-02}
21	—	—	—	0.161×10^{-06}
22	—	—	—	0.315×10^{-06}
23	—	—	—	0.393×10^{-09}
24	—	—	—	0.213×10^{-11}
25	—	—	—	0.189×10^{-19}
26	—	—	—	0.954×10^{-24}

the other hand, the second approach leads to a perfectly well-conditioned formulation in the thin-shell limit, reproduces the results obtained with the classical inextensible director model, and differs from the formulation discussed in Part III by two additional terms that involve the thickness stretch and possess a remarkably simple structure.

On the computational side, we have developed a simple update procedure for the thickness stretch which is exact and ensures that the updated stretch is always positive. In addition, the mixed finite element method of Part III has been extended to include thickness stretch leading to a formulation free from locking in the incompressible limit. The importance of the correct loading terms in the presence of thickness stretch has been emphasized and illustrated by means of a numerical simulation. Our future work will focus on the following three areas.

(i) Exploitation of the present approach in the formulation of three-dimensional hyperelastic constitutive models entirely in stress resultants. This work is already completed and includes models such as Mooney–Rivlin and generalized Ogden materials.

(ii) Formulation and implementation of nonlinear shell theories that include drill rotations. Related work in the context of the linearized theory of elasticity is found in [20, 21]. See also [22] for an alternative approach to nonlinear shells in lines of curvature.
(iii) Formulation and implementation of recently proposed energy and momentum conserving algorithms [23] in the context of dynamic analysis of shells.

Acknowledgment

We wish to thank professors C.R. Steele and R.L. Taylor for many helpful discussions. Support was provided by AFOSR grant nos. 2-DJA-544 and 2-DJA-771 with Stanford University. This support is gratefully acknowledged.

Appendix A. Assumed shear strain formulation

In this appendix, we present the assumed shear strain matrix expressions for the standard formulation presented in Section 4.4. We note, however, that these expressions are nearly identical to those presented in Section 6 of Part II; the only difference between the two presentations is that the inextensible director t is replaced by the extensible director d.

We consider a typical 4-node isoparametric finite element as given by Fig. A.1. The assumed transverse shear strain field is

$$\begin{bmatrix} \tilde{\gamma}_1^h \\ \tilde{\gamma}_2^h \end{bmatrix} = \frac{1}{2} \begin{bmatrix} (1-\eta)\tilde{\gamma}_1^B + (1+\eta)\tilde{\gamma}_1^D \\ (1-\xi)\tilde{\gamma}_2^A + (1+\xi)\tilde{\gamma}_2^C \end{bmatrix}, \tag{A.1}$$

where $\tilde{\gamma}_\alpha^M = \varphi_{,\alpha}^M \cdot d^M$.

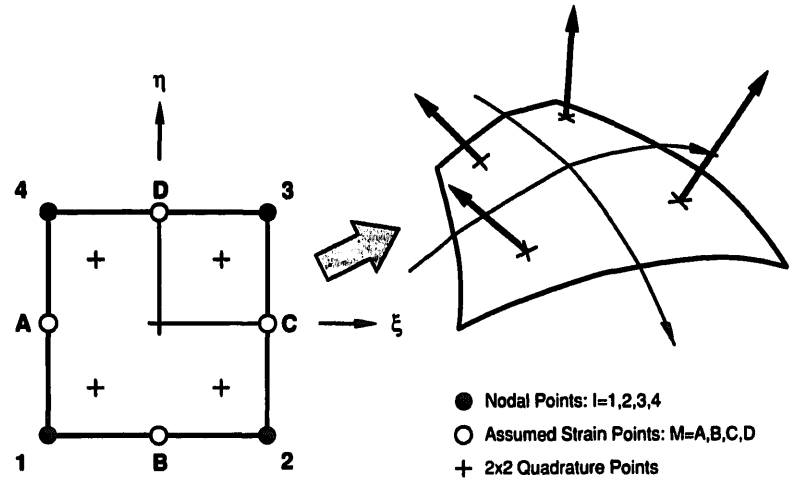

Fig. A.1. Isoparametric bi-unit square. Construction of the assumed strain field.

The shear contribution to the weak form (4.37a) is replaced by

$$\begin{bmatrix} \delta\bar{\tilde{\gamma}}_1^h \\ \delta\bar{\tilde{\gamma}}_2^h \end{bmatrix}_e \cdot \tilde{q} := [\bar{\mathbb{B}}_{sm} \quad \bar{\mathbb{B}}_{sb}] \begin{bmatrix} \delta\varphi_e \\ \delta d_e \end{bmatrix} \cdot \tilde{q}\,, \tag{A.2}$$

where the vectors $\delta\varphi_e$ and δd_e are defined by

$$\delta\varphi_e = \begin{bmatrix} \delta\varphi_1 \\ \delta\varphi_2 \\ \delta\varphi_3 \\ \delta\varphi_4 \end{bmatrix} \quad \text{and} \quad \delta d_e = \begin{bmatrix} \delta d_1 \\ \delta d_2 \\ \delta d_3 \\ \delta d_4 \end{bmatrix}, \tag{A.3}$$

and the discrete shear strain matrices are given by

$$\bar{B}_{sm} := \frac{1}{4}\begin{bmatrix} -(1-\eta)d^{B^t} & (1-\eta)d^{B^t} & (1+\eta)d^{D^t} & -(1+\eta)d^{D^t} \\ -(1-\xi)d^{A^t} & -(1+\xi)d^{C^t} & (1+\xi)d^{C^t} & (1-\xi)d^{A^t} \end{bmatrix}, \tag{A.4}$$

and

$$\bar{B}_{sb} := \frac{1}{4}\begin{bmatrix} (1-\eta)\varphi_{,1}^{B^t} & (1-\eta)\varphi_{,1}^{B^t} & (1+\eta)\varphi_{,1}^{D^t} & (1+\eta)\varphi_{,1}^{D^t} \\ (1-\xi)\varphi_{,2}^{A^t} & (1+\xi)\varphi_{,2}^{C^t} & (1+\xi)\varphi_{,2}^{C^t} & (1-\xi)\varphi_{,2}^{A^t} \end{bmatrix}. \tag{A.5}$$

The contribution of the assumed strain field to the linearization is included in Appendix B, along with the material and geometric tangent stiffness matrices for the standard formulation.

Appendix B. Linearization for standard formulation

In this appendix, we present matrix expressions for the material and the geometric parts of the tangent stiffness which result from substituting isoparametric interpolations (4.40) into the weak form of the balance equations (4.37) for the standard formulation presented in Section 4.4. We denote by B^A the discrete matrix form of the strain operator $\bar{\mathbb{B}}$ obtained from the isoparametric interpolation.

The linearization is split into two parts as

$$DG(\Phi^k; \delta\Phi)\cdot\Delta\Phi = \mathbb{M}(\Phi^k; \delta\Phi, \Delta\Phi) + \mathbb{G}(\Phi^k; \delta\Phi, \Delta\Phi)\,. \tag{B.1}$$

Here, $\mathbb{M}$ and $\mathbb{G}$ are the symmetric bi-linear forms that represent the material and geometric parts of the linearization, respectively. The material contribution is written

$$\mathbb{M}(\Phi^k; \delta\Phi, \Delta\Phi) = \sum_{A=1}^{4}\sum_{B=1}^{4}\int_{\mathscr{A}} [B^A\,\delta\Phi_A]^t C[B^B\,\Delta\Phi_B]\,\bar{j}\,d\xi^1\,d\xi^2\,, \tag{B.2}$$

where B^A is the matrix of discrete strain operators and C is the block-diagonal elasticity matrix defined as follows:

$$B^A = \begin{bmatrix} B_m^A & 0 \\ \bar{B}_{sm}^A & \bar{B}_{sb}^A \\ B_{sm}^A & B_{bb}^A \\ 0 & B_l^A \end{bmatrix}_{11\times 6} \quad \text{and} \quad C = \begin{bmatrix} C_m & & & & \\ & C_s & & & \\ & & C_b & & \\ & & & C_3 & \\ & & & & C_l \end{bmatrix}_{11\times 11} \tag{B.3}$$

The shear contributions to B^A are obtained from

$$\bar{B}_{sm} = [\bar{B}_{sm}^1 \quad \bar{B}_{sm}^2 \quad \bar{B}_{sm}^3 \quad \bar{B}_{sm}^4] \quad , \qquad \bar{B}_{sb} = [\bar{B}_{sb}^1 \quad \bar{B}_{sb}^2 \quad \bar{B}_{sb}^3 \quad \bar{B}_{sb}^4] , \tag{B.4}$$

where $\bar{B}_{sm}^A$ and $\bar{B}_{sb}^A$, for $A = 1, 2, 3, 4$ are the 2×3 matrix contributions obtained from (A.4) and (A.5).

The geometric part of the tangent operator is denoted symbolically by

$$\mathbb{G}(\Phi^k; \delta\Phi, \Delta\Phi) = \int_{\mathscr{A}} [\tilde{n}^{\alpha\beta}\, \Delta(\tfrac{1}{2}\delta a_{\alpha\beta}) + \tilde{q}^{\alpha}\, \Delta(\delta\tilde{\gamma}_{\alpha}) + \tilde{m}^{\alpha\beta}\, \Delta(\delta\tilde{\kappa}_{\alpha\beta}) + \tilde{m}^{3\alpha}\, \Delta(\delta\tilde{\mu}_{\alpha}) + \tilde{l}^{3}\, \Delta(\tfrac{1}{2}\delta(\lambda^2))]\, \bar{j}\, d\xi^1\, d\xi^2 , \tag{B.5}$$

where the individual contributions are given by

$$\begin{aligned}
\tilde{n}^{\alpha\beta}\, \Delta(\tfrac{1}{2}\delta a_{\alpha\beta}) &= \sum_{A=1}^{4} \sum_{B=1}^{4} \delta\varphi_A^{t} [\tilde{n}^{\alpha\beta} N_{,\alpha}^A B_{,\beta}^B 1]\, \Delta\varphi_B , \\
\tilde{m}^{\alpha\beta}\, \Delta(\delta\tilde{\kappa}_{\alpha\beta}) &= \sum_{A=1}^{4} \sum_{B=1}^{4} \{\delta\varphi_A^{t} [\tilde{m}^{\alpha\beta} N_{,\alpha}^A N_{,\beta}^B 1]\, \Delta d_B + \delta d_A^{t} [\tilde{m}^{\alpha\beta} N_{,\beta}^A N_{,\alpha}^B 1]\, \Delta\varphi_B\} , \\
\tilde{m}^{3\alpha}\, \Delta(\delta\tilde{\mu}_{\alpha}) &= \sum_{A=1}^{4} \sum_{B=1}^{4} \delta d_A^{t} [\tilde{m}^{3\alpha} (N_{,\alpha}^A N^B + N_{,\alpha}^B N^A) 1]\, \Delta d_B , \\
\tilde{l}^{3}\, \Delta(\tfrac{1}{2}\delta(\lambda^2)) &= \sum_{A=1}^{4} \sum_{B=1}^{4} \delta d_A^{t} [\tilde{l}^{3} N^A N^B 1]\, \Delta d_B .
\end{aligned} \tag{B.6}$$

Due to the assumed shear strain field, the shear contribution to the geometric tangent operator becomes

$$\tilde{q}^{\alpha}\, \Delta(\delta\tilde{\gamma}_{\alpha}) = \begin{bmatrix} \delta\varphi_1 \\ \delta\varphi_2 \\ \delta\varphi_3 \\ \delta\varphi_4 \end{bmatrix}^{t} A \begin{bmatrix} \Delta d_1 \\ \Delta d_2 \\ \Delta d_3 \\ \Delta d_4 \end{bmatrix} + \begin{bmatrix} \delta d_1 \\ \delta d_2 \\ \delta d_3 \\ \delta d_4 \end{bmatrix}^{t} A^{t} \begin{bmatrix} \Delta\varphi_1 \\ \Delta\varphi_2 \\ \Delta\varphi_3 \\ \Delta\varphi_4 \end{bmatrix} , \tag{B.7}$$

where the matrix A is given by

$$A = \frac{1}{8} \begin{bmatrix} [-\tilde{q}^1(1-\eta) - \tilde{q}^2(1-\xi)]1 & -\tilde{q}^1(1-\eta)1 & 0 & -\tilde{q}^2(1-\xi)1 \\ \tilde{q}^1(1-\eta)1 & [\tilde{q}^1(1-\eta) - \tilde{q}^2(1+\xi)]1 & -\tilde{q}^2(1+\xi)1 & 0 \\ 0 & \tilde{q}^2(1+\xi)1 & [\tilde{q}^1(1+\eta) + \tilde{q}^2(1+\xi)]1 & \tilde{q}^1(1+\eta)1 \\ \tilde{q}^2(1-\xi)1 & 0 & -\tilde{q}^1(1+\eta)1 & [-\tilde{q}^1(1+\eta) + \tilde{q}^2(1-\xi)]1 \end{bmatrix} . \tag{B.8}$$

References

[1] J.C. Simo and D.D. Fox, On a stress resultant geometrically exact shell model, Part I: Formulation and optimal parametrization, Comput. Methods Appl. Mech. Engrg. 72 (1989) 267–304.
[2] J.C. Simo, D.D. Fox and M.S. Rifai, On a stress resultant geometrically exact shell model, Part II: The linear theory; Computational aspects, Comput. Methods Appl. Mech. Engrg. 73 (1989) 53–92.
[3] J.C. Simo, D.D. Fox and M.S. Rifai, On a stress resultant geometrically exact shell model, Part III: Computational aspects of the nonlinear theory, Comput. Methods Appl. Mech. Engrg. 79 (1990) 21–70.
[4] F.B. Hildebrand, E. Reissner and G.B. Thomas, Notes on the foundations of the theory of small displacements of Orthotropic shells, National Advisory Committee for Aerodynamics, Technical Note No. 1833, 1949.
[5] A.E. Green and W. Zerna, The equilibrium of thin elastic shells, Quat. J. Mech. Appl. Math. III (1950) 9–22.
[6] P.M. Naghdi, The theory of shells, in: C. Truesdell, Ed., Handbuch der Physik, Vol. Via/2, Mechanics of Solids II (Springer, Berlin, 1972).
[7] E. Reissner, On finite axi-symmetrical deformations of thin elastic shells of revolution, J. Comput. Mech. (1989) to appear.
[8] S.S. Antman, Ordinary differential equations of nonlinear elasticity I: Foundations of the theories of non-linearly elastic rods and shell, Arch. Rat. Mech. Anal. 61 (4) (1976) 307–351.
[9] A.E. Green, P.M. Naghdi and M.L. Wenner, Linear theory of Cosserat surface and elastic plates of variable thickness, Proc. Camb. Phil. Soc. 69 (1971) 227–254.
[10] S.S. Antman, Existence and nonuniqueness of axisymmetric equilibrium states of nonlinearly elastic shells, Arch. Rat. Mech. Anal. 40 (5) (1971) 329–372.
[11] T.J.R. Hughes and E. Carnoy, Nonlinear finite element shell formulation accounting for large membrane strains, Comput. Methods. Appl. Mech. Engrg. 39 (1983) 69–82.
[12] J.C. Simo and J.G. Kennedy, On a stress resultant geometrically exact shell model. Part V: Nonlinear plasticity. Formulation and integration algorithms, Comput. Methods Appl. Mech. Engrg., submitted.
[13] T.J.R. Hughes, The Finite Element Method (Prentice-Hall, Englewood Cliffs, NJ, 1987).
[14] O.C. Zienkiewicz and R.L. Taylor, The Finite Element Method. Vol I: Linear Analysis (McGraw-Hill, New York, 1989).
[15] D.P. Bertsekas, Constrained Optimization and Lagrange Multiplier Methods (Academic Press, New York, 1982).
[16] J.C. Simo and R.L. Taylor, Finite elasticity in principal stretches: Formulation and augmented Lagrangian algorithms.
[17] A.C. Scordellis and K.S. Lo, Computer analysis of cylindrical shells, J. Am. Concr. Inst. 61 (1969) 539–561.
[18] L.S.D. Morely, Skew plates and structures, Internat. Series of Monographs in Aeronautics and Astronautics (MacMillan, New York, 1963).
[19] L.S.D. Morely and A.J. Morris, Conflict between finite elements and shell theory, Royal Aircraft Establishment Report, London, 1978.
[20] E. Reissner, A note on variational theorems in elasticity, Internat. J. Solids and Structures 1 (1965) 93–95.
[21] T.J.R. Hughes and F. Brezzi, On drilling degrees of freedom, Comput. Methods Appl. Mech. Engrg. 72 (1989) 105–121.
[22] E. Reissner, A note on two-dimensional finite-deformation theories of shells, Internat. J. Non-Linear Mech. 17 (3) (1982) 217–221.
[23] J.C. Simo and K. Wong, Unconditionally stable algorithms for the orthogonal group that exactly preserve energy and momentum (preprint 1989).
[24] L.A. Taber, Large deflection of a fluid-filled spherical shell under a point load, J. Appl. Mech. 49 (1982) 121–128.